FINAL REPORT

PROJECT N00014-08-1-0180

Attn: Don Hoffman
Office of Naval Research
ONR Code 331
875 North Randolph St, Suite 1425
Arlington, VA 22203-1995

HIGH SPEED TURBO-GENERATOR: TEST STAND SIMULATOR INCLUDING TURBINE ENGINE EMULATOR

30 July 2010
Revised May 13 2011

Submitted by:
Dr. Roger A. Dougal, PI
Blanca Correa
Dr. Yucheng Zhang
Richard Smart

with contributions by
Dr. Jamil Khan, Co-PI
Dr. Anton Smith
Dr. Wei Jiang
Ruixian Fang
College of Engineering
University of South Carolina

Technical POC

Dr. Roger Dougal
Dept. of Electrical Engineering
University of South Carolina
Columbia, SC 29208
Telephone: (803) 777-7890
Fax: (803) 777-8045
email: dougal@engr.sc.edu

Administrative POC

Danielle McElwain
Sponsored Awards Management
901 Sumter Street
Columbia, SC 29208
Telephone: (803) 777-1119
Fax: (803) 777-4136
email: dmcelwai@mailbox.sc.edu

REPORT DOCUMENTATION PAGE

Form Approved
OMB No. 0704-0188

1. REPORT DATE *(DD-MM-YYYY)*	2. REPORT TYPE	3. DATES COVERED *(From - To)*
05-12-2010	Final Technical	11/7/2007-4/30/2010

4. TITLE AND SUBTITLE
HIGH SPEED TURBO-GENERATOR: TEST STAND SIMULATOR INCLUDING TURBINE ENGINE EMULATOR

5a. CONTRACT NUMBER

5b. GRANT NUMBER
N00014-08-1-0180

5c. PROGRAM ELEMENT NUMBER

6. AUTHOR(S)
Dr. Roger A. Dougal, PI, Blanca Correa, Richard Smart
Dr. Jamil Khan, Co-PI, Dr. Anton Smith, Dr. Wei Jiang, Ruixian Fang

5d. PROJECT NUMBER

5e. TASK NUMBER

5f. WORK UNIT NUMBER

7. PERFORMING ORGANIZATION NAME(S) AND ADDRESS(ES)
Dept. of Electrical Engineering
University of South Carolina
301 South Main Street
Columbia, SC 29208

8. PERFORMING ORGANIZATION REPORT NUMBER

9. SPONSORING/MONITORING AGENCY NAME(S) AND ADDRESS(ES)
Office of Naval Research
ONR Code 331
875 North Randolph St, Suite 1425
Arlington, VA 22203-1995

10. SPONSOR/MONITOR'S ACRONYM(S)
ONR

11. SPONSORING/MONITORING AGENCY REPORT NUMBER

12. DISTRIBUTION AVAILABILITY STATEMENT
Approved for Public Release; Distribution is Unlimited.

13. SUPPLEMENTARY NOTES

14. ABSTRACT
Our research developed: a reference model of a turbo-generator system, a control model of the high speed generator test stand, and a model of a high speed generator test stand (including controls) that uses an electric machine to drive the generator as though it were being driven by the gas turbine engine. The performance of our gas turbine model was compared to that predicted by a validated commercial gas turbine simulation software and the two agreed well for operation near the design point. Agreement was less good when operating off the design point, for reasons that are well understood and are attributed to simplifications in our model. A model-based controller schema was adopted to control the synchronous motor so that it emulates the torque-speed characteristics of the gas turbine engine. Excellent agreement was found when comparing the performance of the reference system to the performance of the gas turbine emulator system when both were subjected to changes of the electrical load on the generator.

15. SUBJECT TERMS
High speed turbo-generator, Gas turbine emulator, Generator test stand

16. SECURITY CLASSIFICATION OF:			17. LIMITATION OF ABSTRACT	18. NUMBER OF PAGES	19a. NAME OF RESPONSIBLE PERSON
a. REPORT	b. ABSTRACT	c. THIS PAGE			19b. TELEPONE NUMBER *(Include area code)*

EXECUTIVE SUMMARY

The purpose of this research was to support the capability of NSWC Philadelphia to test high speed turbo generators. Our research developed 1) a reference model of a turbo-generator system, 2) a control model of the high speed generator test stand, and 3) a model of a high speed generator test stand (including controls) that uses an electric machine to drive the high speed generator as though it were being driven by the gas turbine engine.

The system models and the controls were developed in the Virtual Test Bed (VTB 2009) software environment. In order to develop the three system models, it was first necessary to design and build component models of the gas turbine engine, the six phase generator, and the driving motor. A new flexibly-controllable model of a resistive load was also developed to simplify user interaction with the generator loads during simulation runtime.

The performance predicted by our gas turbine model was compared to that predicted by a validated commercial gas turbine simulation software and the two agreed well for operation near the design point of the engine. Agreement was less good when operating off the design point, for reasons that are well understood and are attributed to simplifications in our model that will be improved in later versions. Our model shows that a properly-rated motor generator system can respond to load changes faster than can a turbo-generator system, and so a motor generator test stand can accurately emulate a gas turbine generator system.

A model-based controller schema was adopted to control the synchronous motor so that it emulates the torque-speed characteristics of the gas turbine engine. In this schema, a model of the gas turbine engine uses the torque demand of the generator to compute the speed reference for the drive motor. This control approach was tested by comparing the performance of the reference system to the performance of the gas turbine emulator system when both were subjected to step changes of the electrical load on the generator. Excellent agreement was found: the emulator motor speed displayed the same transient response as was predicted by the reference model of the turbogenerator system. Speed oscillations were slightly larger for the emulator system, however, the greatest error never exceeded 0.09 percent.

Our research also defined the power-inertia relationship that is required in order for a relatively-high-inertia electric machine to emulate the performance of a relatively-low-inertia gas turbine engine. We plan to validate that relationship on a small-scale hardware testbed and, after validation, we will use the relationship to define the scope of tests that can be productively accomplished at NSWC Philadelphia, considering the ratings of the machinery installed there.

Towards the end of our report, we recommend specific enhancements to our models and additional simulation studies that should be performed using the models. We plan to conduct small scale hardware verification of the emulator control and of the derived power requirement. Finally, we note that our work is limited by a lack of detailed knowledge of the actual equipment and controls installed at NSWC Philadelphia, and of any specific gas turbine engine configuration. .

TABLE OF CONTENTS

INTRODUCTION

This report documents the research performed under Office of Naval Research grant # N00014-08-1-0180, "High Speed Turbo-Generator: Test Stand Simulator including Turbine Engine Emulator." We present the working principles, simulation models and simulation results for two system models that we developed to address a need by the Naval Surface Warfare Center, Philadelphia (NSWC Philadelphia). NSWC Philadelphia intends to develop a capability for testing high speed turbo-generators. To minimize cost, the initial system will use an existing AC electric motor to drive the high speed generator, in place of a gas turbine engine. The electric motor should simulate the speed-torque characteristic of the gas turbine in order to study the operation of the turbo-generator system.

For this research we developed three system models and the associated controls:

1. Gas turbine powered generator system with user-adjustable speed reference
2. Motor driven generator system with user-adjustable speed reference
3. Motor-driven generator system and model-based controls that permit it to emulate the gas turbine generator system

The first system model, illustrated in **Error! Reference source not found.**, represents the turbo-generator system of interest, and serves as the reference for the studies performed. In order to construct this system model, we designed and built component models for the gas turbine engine and a six phase generator. We developed a fuel control for the gas turbine that varies the fuel input so that the model exhibits appropriate speed-torque characteristics. We also developed a controllable resistive electrical load that provides a convenient means to exercise the system models.

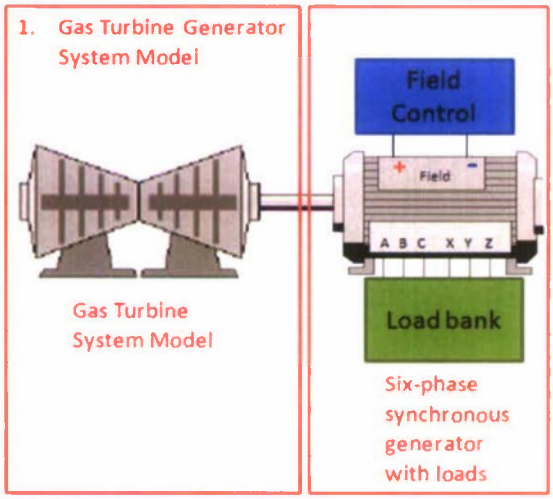

Figure 1: Illustration of gas turbine generator system having gas turbine, high speed generator, and loads

The second system model, illustrated in **Error! Reference source not found.**, conforms to the configuration of the hardware that is expected to be installed at NSWC Philadelphia; it represents a motor drive supplying a synchronous motor driving a synchronous generator

through a gearbox. This system model uses the same generator and load models as were used in the gas turbine generator system model. The speed referenee for the vector-controlled motor drive is assigned by the user. It should be possible to validate this model against experimental data taken from the NSWC test stand, when available. This model permits study, and predietion of system performanee when the motor is operating under user eontrol and not as a gas turbine emulator.

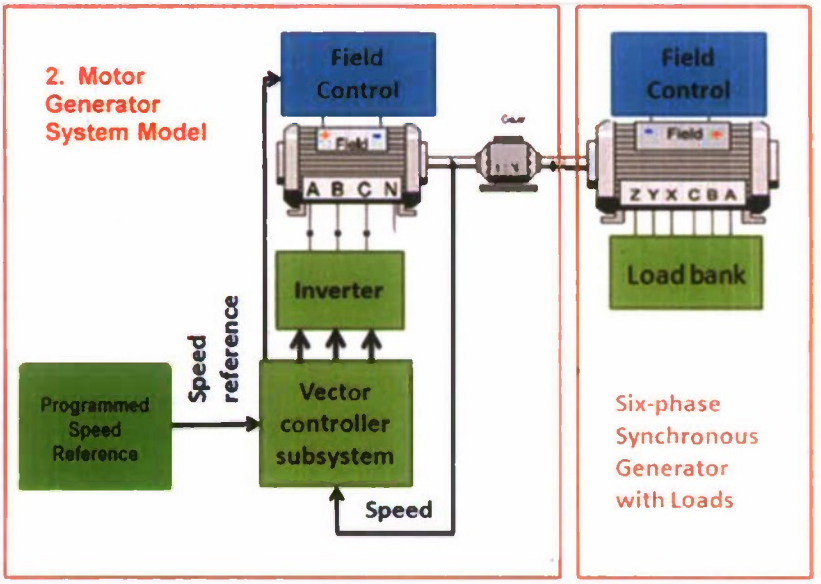

Figure 2: Illustration of motor generator system having synchronous motor with a programmed speed reference, high speed generator, and loads

The third system model, Figure 3, represents the motor-generator system of Figure 2 when it is eonfigured to operate in gas turbine emulation mode. This system model uses the same synchronous motor, generator and load models as the motor generator system model, and it is augmented with a gas turbine engine model that provides the speed referenee for the synehronous motor so that the motor behaves like the gas turbine engine. This gas turbine emulator mode of operation will be useful for planning and vetting dynamie tests of the high speed generator operating in turbine emulation mode, for generating referenee data for comparison to experimental data, and for studying in some detail the dynamics of the systems. The model ean be adapted for use in real-time mode in a elosed-loop feedbaek eontrol for the aetual turbine emulator maehine.

The simulation models were designed and implemented in the Virtual Test Bed (VTB 2009) software, whieh is a eomprehensive simulation and virtual prototyping environment for advaneed power systems developed at the Department of Eleetrieal Engineering from the University of South Carolina.

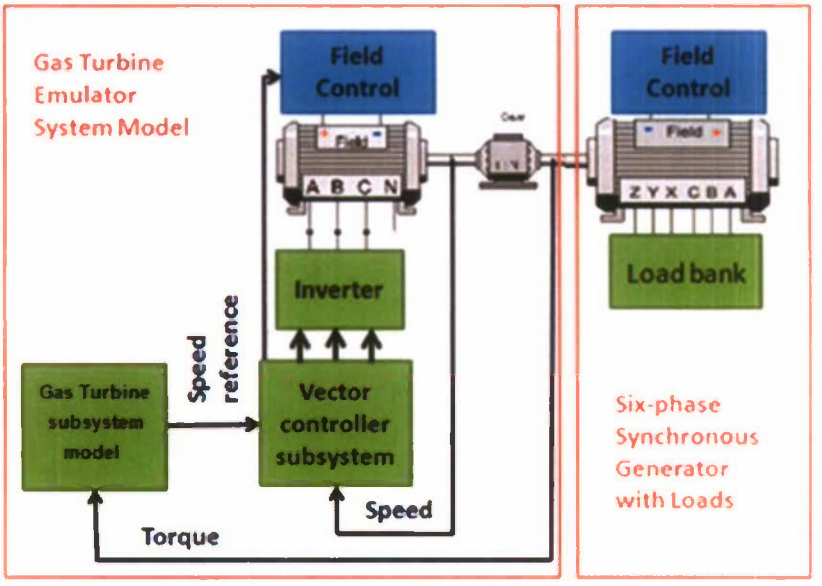

Figure 3: Illustration of gas turbine emulator system having synchronous motor with a programmed speed reference, high speed generator, and loads

DESIGN PARAMETERS

The nominal parameters for the high speed generator, prospective gas turbine engine, and turbine emulator drive motor are:

1. High Speed Gencrator – Six-phase synchronous gencrator configured to run at 6000-12000 rpm, and produce 8-14 MW power at 6.6 kV
2. Gas Turbine – Two shaft gas turbine operating at 6000-12000 rpm and producing nominally 10-14 MW power.
3. Gas Turbine Emulator drive machine implemented as a synchronous motor having nominal rated power of 26.25 MW, at rated speed of 3600 rpm on 4.16 kV 60 Hz power driven by a vector controlled motor drive

SYSTEM MODELS

Reference model of the Turbine Engine Powered Generator System

The reference model of the system that we seek to emulate, a two-shaft gas turbine powering a synchronous generator, is illustrated in Figure 4. The gas turbine subsystem consists of compressors and turbine on one shaft and a power takeoff turbine on a second shaft. The model is based on the working principles of a simple-cycle, two-shaft gas turbine with intercooler. A two-stage compressor increases air pressure from 1 to 15 bar. An intercooler cools the air between the compressor stages to improve compression efficiency. The compressed air and fuel are channeled to the combustor between the 2nd compressor stage and the 1st turbine. The high temperature exhaust gas expands through two turbine stages. The power generated by the 1st gas turbine is fully consumed by the compressors. Subsequent gas expansion through the air coupled power turbine produces mechanical power to drive the high speed generator. The turbine subsystem also includes a motor for start-up, which is cut off automatically after reaching a specific rotational speed. Speed, fuel, and temperature controls are included. The major component models of this system are described in Appendix A.

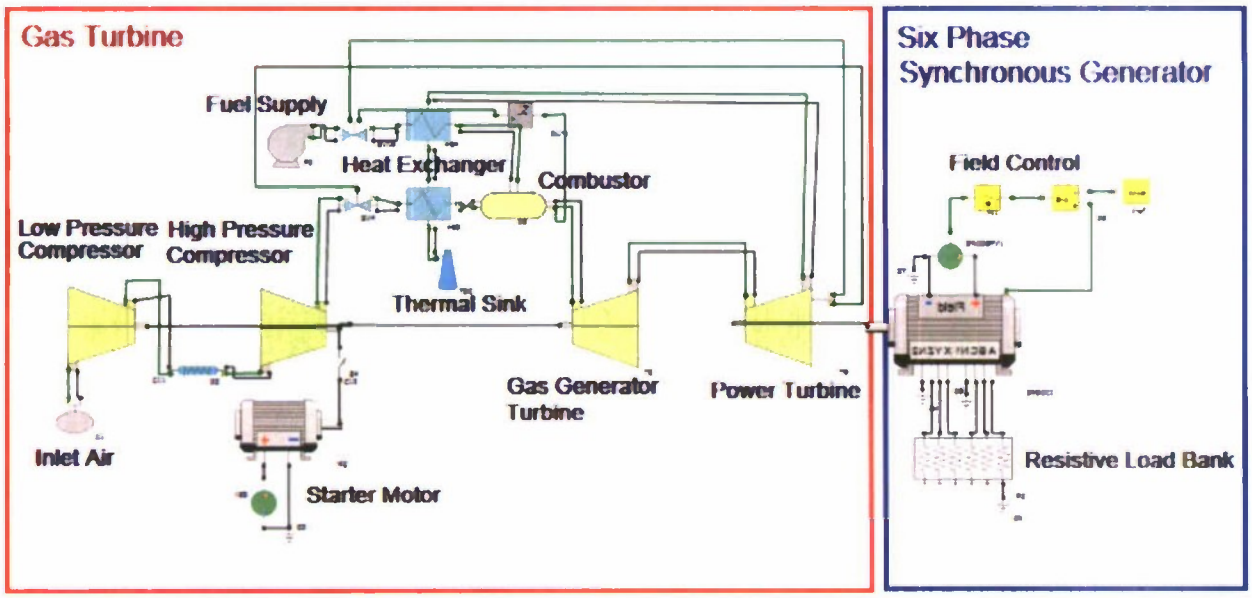

Figure 4: Gas turbine generator system model

The speed vs. torque relationship produced by the gas turbine model is shown in Figure 5. It can be observed that for the constant rotational speed command of 854 rad/sec (~8.1k rpm), the speed remains constant as the torque increases, up to 26920 N*m. At that point, the maximum fuel supply for the gas turbine has been reached, and the system produces its maximum power. As torque load is increased further, the speed decreases. The speed vs. torque curves for commanded speeds of 754 and 654 rad/sec (7.2k and 6.2k rpm) present similar trends. As shown in **Error! Reference source not found.** for operation of the gas turbine at 754 rad/s, the fuel flow rate varies linearly with the power turbine output power. The maximum fuel flow rate (0.8 kg/s) is reached at maximum power (22.7MW).

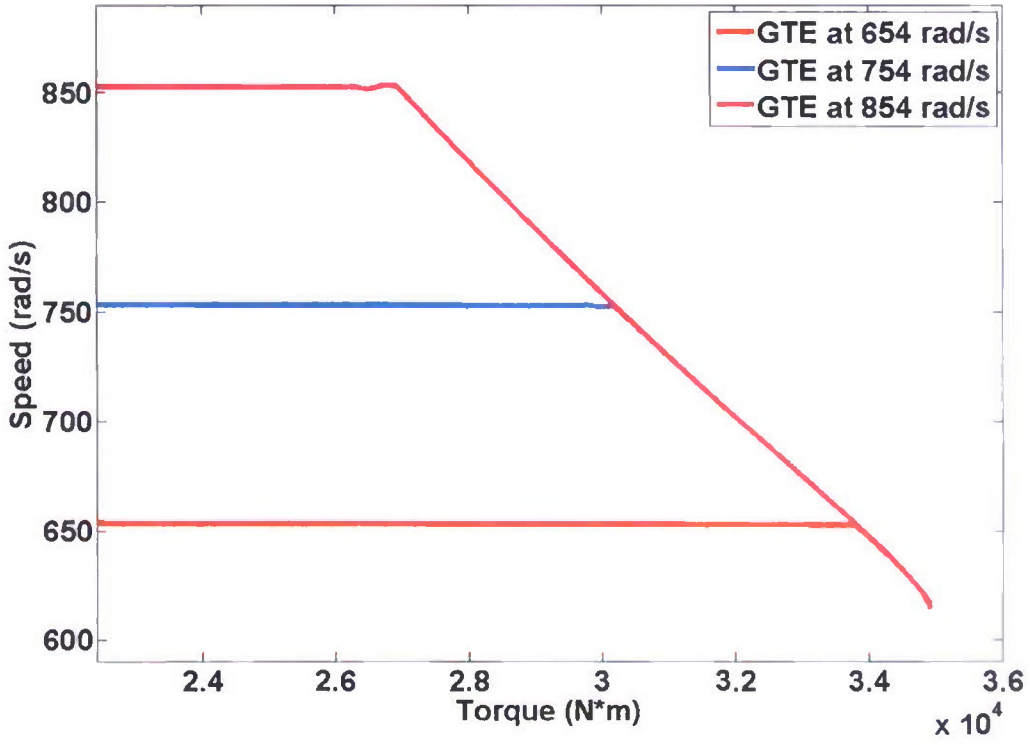

Figure 5: Speed vs. torque characteristic of gas turbine

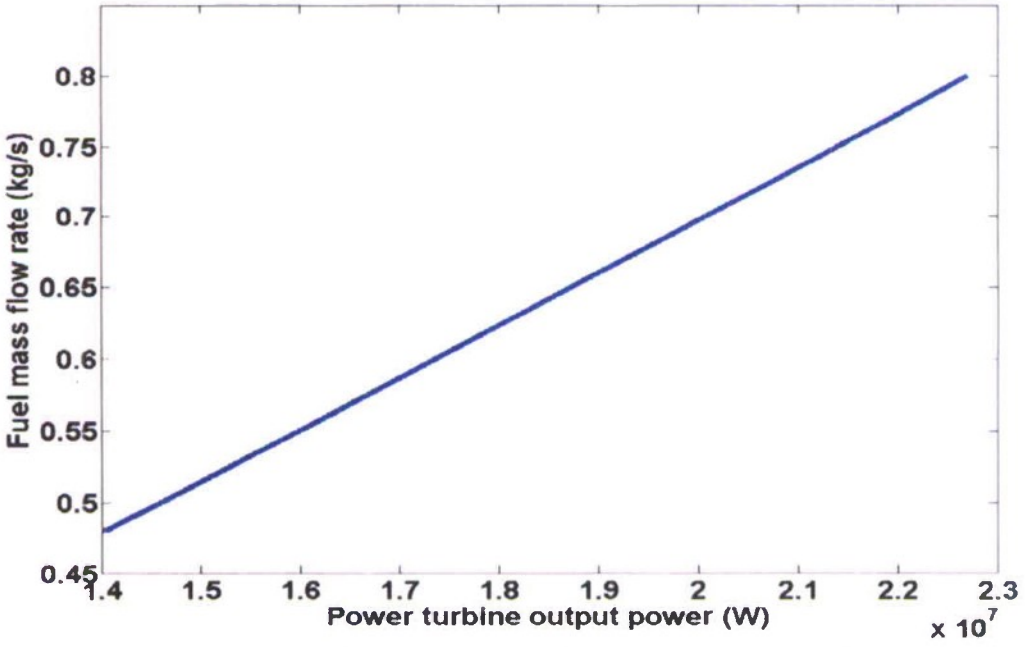

Figure 6: Fuel mass flow vs. power turbine output power when operating at 754 rad/s

In the absence of actual and specific engine data against which to validate these trend lines, we compared the performance of our gas turbine engine model to that of a similarly paramaterized model in the commercial gas turbine performance modeling software GasTurb 11. Table 1 shows the differences between the results produced by the GasTurb 11 and VTB simulations. The performance of our model is acceptable when the model is operated at its design point, but poorer when operating off the design point. At the design point, the small differences between the models are attributable to the assumption of ideal compression in our model. Off the design point, our model is less good because we simply shift the reference compressor characteristic curve to the new speed point, rather than change the shape of the compressor curve as should actually be done. We anticipate refining our model in the future so that it better represents the full compressor map. This should mitigate the off-design point errors.

Table 1: Comparison of Simulation Results for GasTurb 11 and VTB Gas Turbine Component Models

	Percent Difference between GasTurb 11 and VTB Models	
	At Design Point	**Off-Design Point (speed 10% below design point)**
Compressor		
Outlet pressure	**2%**	**42%**
Outlet temperature	**9%**	**0%**
Turbine		
Outlet pressure	**4%**	**9%**
Outlet temperature	**8%**	**15%**
Shaft Power	**4%**	**8%**

Our model of the six-phase synchronous machine was based on work by Schiferl and Ong [1]. The six-phase synchronous machine is described mathematically by dividing the six stator phases into two three-phase sets displaced by an angle ε, and labeled *abc* and *xyz*. The model considers the effects of two damper windings. Figure 7 shows a schematic representation of the two stator windings, field winding and damper windings. The machine also includes two grounding ports. A more complete description of the generator model is included in Appendix B.

It is assumed that phase *x* voltage is displaced by 60 degrees from phase *a* voltage which has 0 degree phase reference when field current flows into the field plus terminal. Phase *b* lags phase *a* by 120 degrees and phase *c* leads phase *a* by 120 degrees. Similarly, phase *y* lags phase *x* by 120 degrees and phase *z* leads phase *x* by 120 degrees.

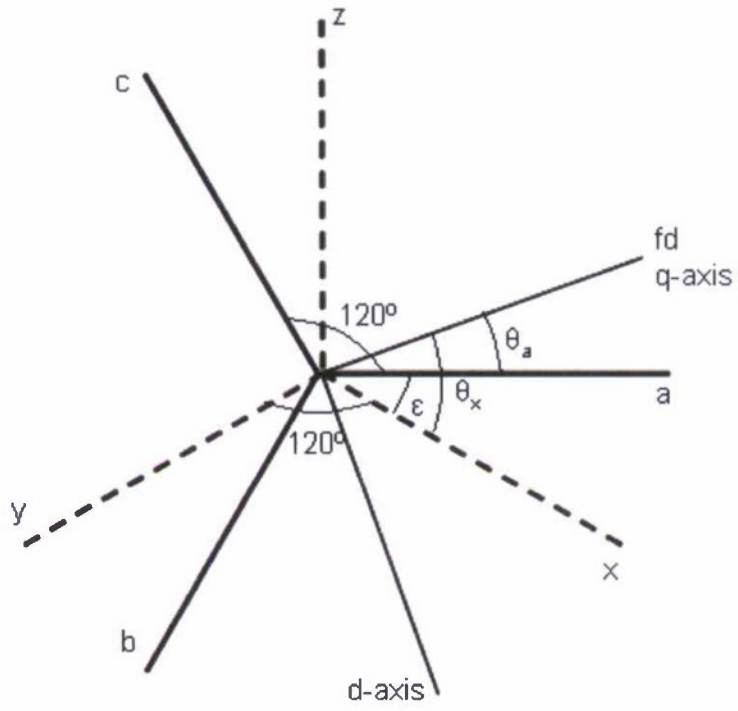

Figure 7: Schematic representation of the two stator windings, field winding and damper windings for six-phase generator

Model of the Motor, Gearbox, High Speed Generator System

The motor generator system model uses the same generator and load subsystems as were previously described but now the turbine engine model is replace by a model of a synchronous motor that drives the generator via a 1:2 mechanical gear that increases the shaft speed of the motor to the speed range of the turbine engine. The model of the synchronous motor, described in Appendix C, is based on a dq reference frame approach for a 3-phase system. The model has ABC terminals to connect to the electrical system. It also has an excitation winding on the D axis and three damping windings, one on the D axis and two on the Q axis. The parameters of the synchronous motor are given in Table 2. All the parameters with exception of the transient and subtransient open-circuit (O.C.), and transient and subtransient short-circuit (S.C.) time constants were provided by the sponsor. These time constants were assumed based on documentation provided by Brush Company for a synchronous machine with equal power rating but with line voltage of 13.8 kV.

Table 2: Synchronous motor standard parameters

Line voltage (rms)	4.16kV
Frequency	60 Hz
Rated Speed	3600 rpm
Power	26.25MVA
Inertia	551 kg*m^2
Synchronous reactance	2.08 pu
Saturated transient reactance	0.324 pu
Saturated subtransient reactance	0.25 pu
Unsaturated negative sequence reactance	0.268 pu
Unsaturated zero sequence reactance	0.125 pu
Transient O.C. time constant	7.2s
Transient S.C. time constant	0.85s
Subtransient O.C. time constant	0.05s
Subtransient S.C. time constant	0.04s
Rs	0.0129 Ω

The synchronous motor installed at NSWC Philadelphia controller is powered through a two-quadrant Robicon drive that only allows forward and reverse motoring; it does not permit regeneration. This significantly impacts the ability of the system to emulate the dynamic response of a gas turbine engine under some operating conditions, but not the ability to emulate the steady-state response. Since detailed technical information about this drive and particularly about the internal controls of the drive, were not available, we developed a model that represents a drive that is typical of those used for large synchronous motors. Our model is currently configured as a four quadrant drive that permits both motoring (putting energy into the system) and regeneration (extracting energy from the system) in both directions. Of course gas turbines rotate only in one direction so two of the four operating quadrants should never be exercised.

We implemented a speed control for the synchronous motor by using a vector control scheme based on the works of Bose, and Matuonto and A. Monti ([2], [3]). The control, shown in Figure 8, consists of a two-loop structure: the outer loop is the speed controller, the output of which is the reference value of the torque T_e, and the inner loop is the current control which tries to follow the reference currents produced by the outer loop. A flux controller and a field current controller control the magnetization of the emulator motor. The control is designed so that the motor speed tracks the user programmed reference speed ω_r^*. A more complete description of the control schema is presented in Appendix D.

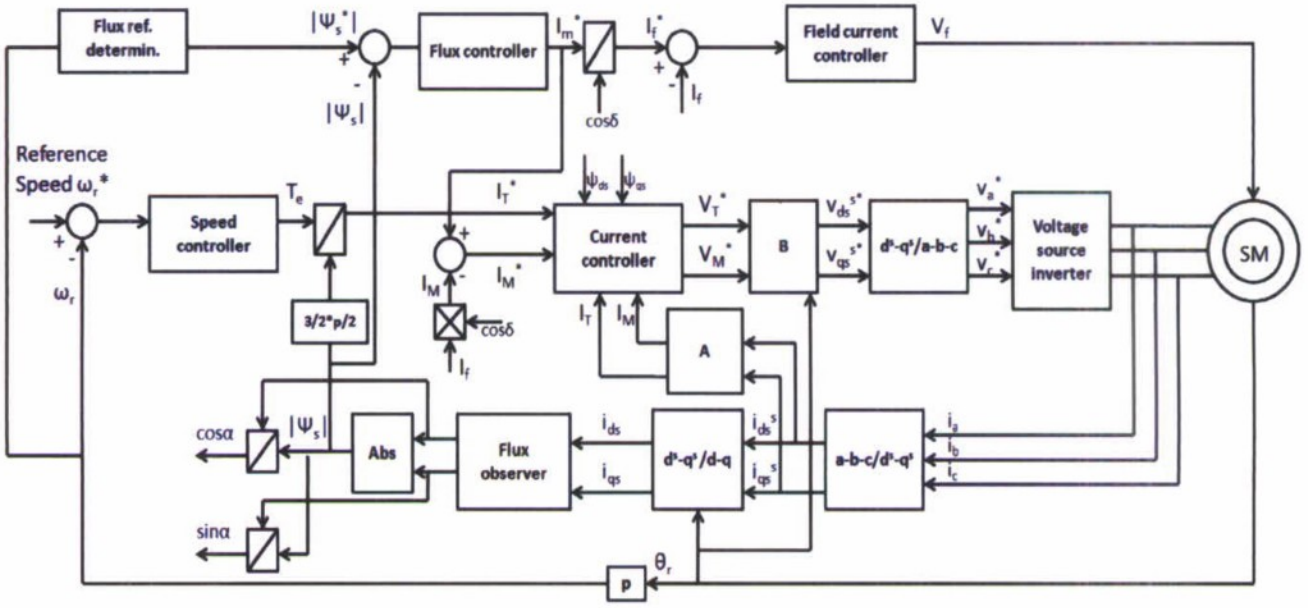

Figure 8: Vector control scheme of the synchronous motor

Simulations verified that the motor and controller performed as intended in steady state. The speed control maintained the motor speed at the 377 rad/s (3600 RPM) setpoint, the magnetization current reference I_M^* remained near zero during steady state operation as expected for a vector controller, and that the machine was able to drive a load torque on the order of 69500 N*m and produce the required shaft power of 26.25 MW (see Figure 9). Data are not available to permit a comparison of emulator model simulations with actual performance of the NSWC Philadelphia motor and drive.

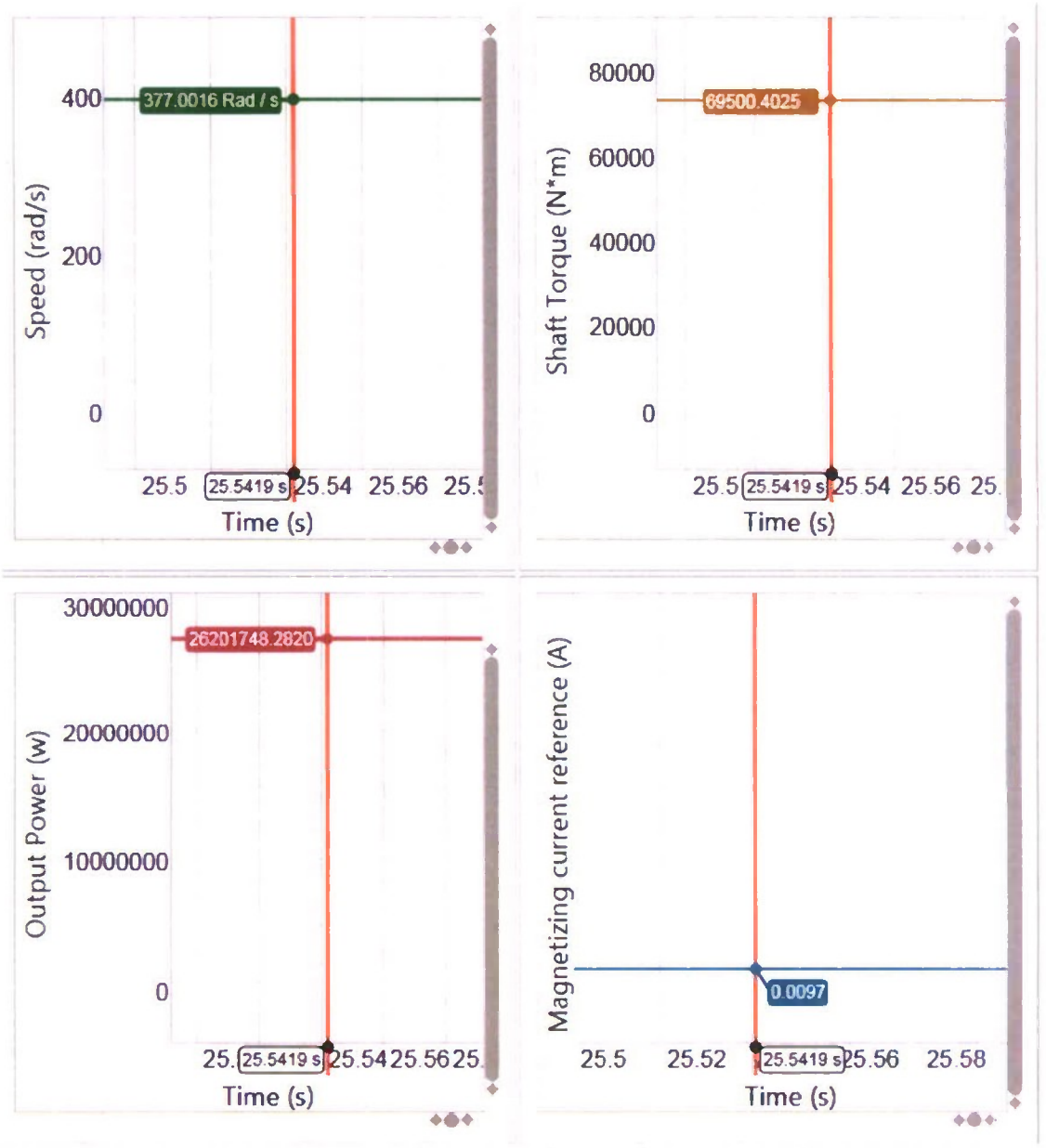

Figure 9: Gas turbine emulator simulation showing steady state motor speed, shaft torque, output power and I_M^*

Transient response of gas turbine generator and motor generator system models

First, we examincd the responsc of the gas turbinc driven generator system to transicnt electrical loads. To do this we applied a step load change to the generator and considered two response characteristics: the speed deviation and the settling time. These response characteristics were later compared to characteristics of the emulator system models. Thcse response characteristics are defined as follows:

- Speed Deviation: Maximum variation of shaft speed from thc nominal shaft speed after a perturbation of the electrical load.

- Settling Time: Time from application of a load perturbation to the time when the shaft speed is 36% of the maximum peak excursion.

The upper plot in Figure 10 shows the generator shaft speed as a function of time following application of a 20% step load decrease to the generator. When the load is decreased, the shaft speed initially increases as expected, because the gas turbine fuel control does not act instantaneously. The speed oscillates for several cycles as the fuel control works to bring the system back to the reference speed. The settling time remains almost invariable (0.53s) between different sizes of load step changes applied. The response to a step load increase is similar, but initially the shaft speed decreases, rather than increases.

The lower plots in Figure 10 show the speed deviation (left) and the settling time (right) as a function of the size of the load step-down. It is observed that the maximum speed deviation increases as the load step increases. The settling time is relatively constant for load decreases between 10% and 50% of rated power showing the invariability in this system characteristic.

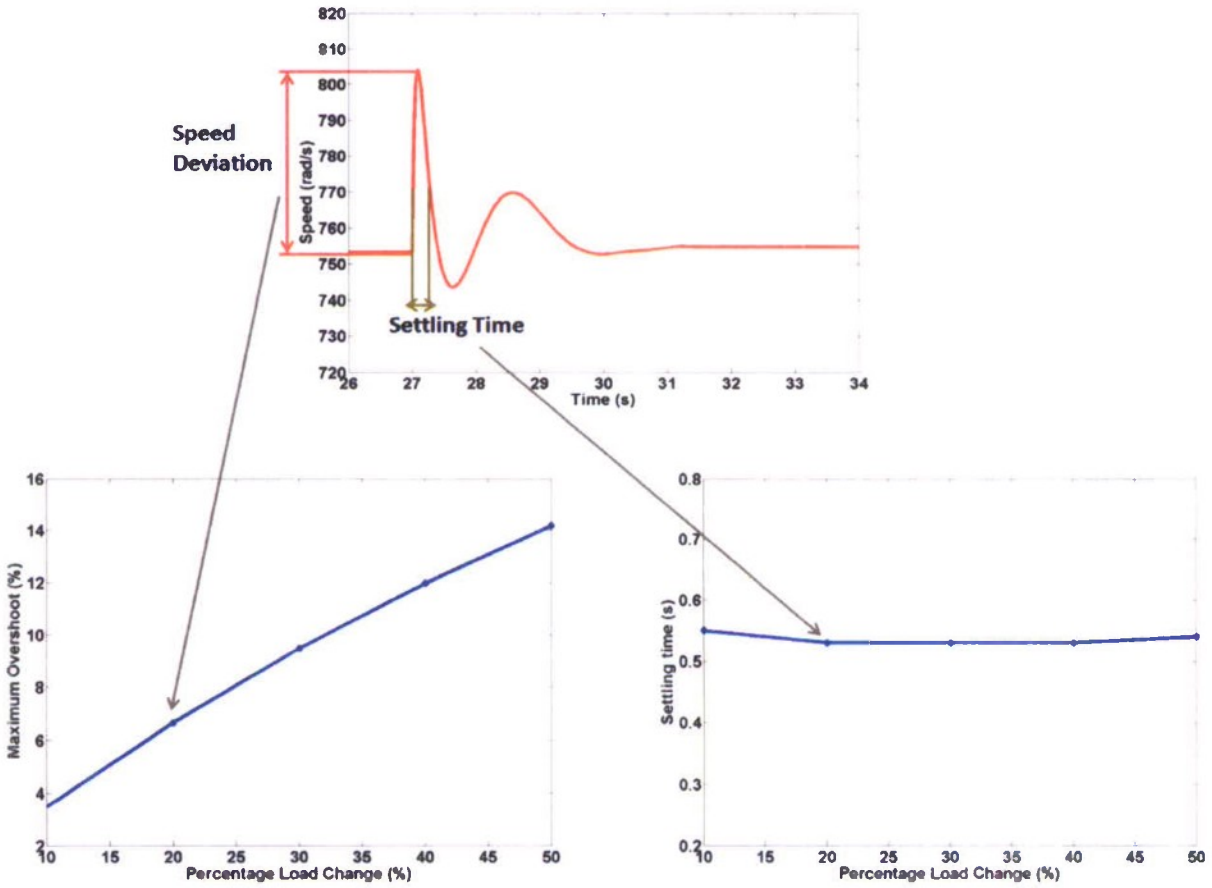

Figure 10: Gas turbine system model response to load perturbation

Figure 11 shows the maximum speed deviation and the settling time as a function of magnitude of the load decrease when operating the gas turbine generator system at 70% of nominal load. In this case, the maximum speed deviation and the settling time present slightly larger values compared to the nominal case shown in Figure 10. Similar to the previous case, the settling time is relatively constant (0.58s) for load decreases between 10% and 50%.

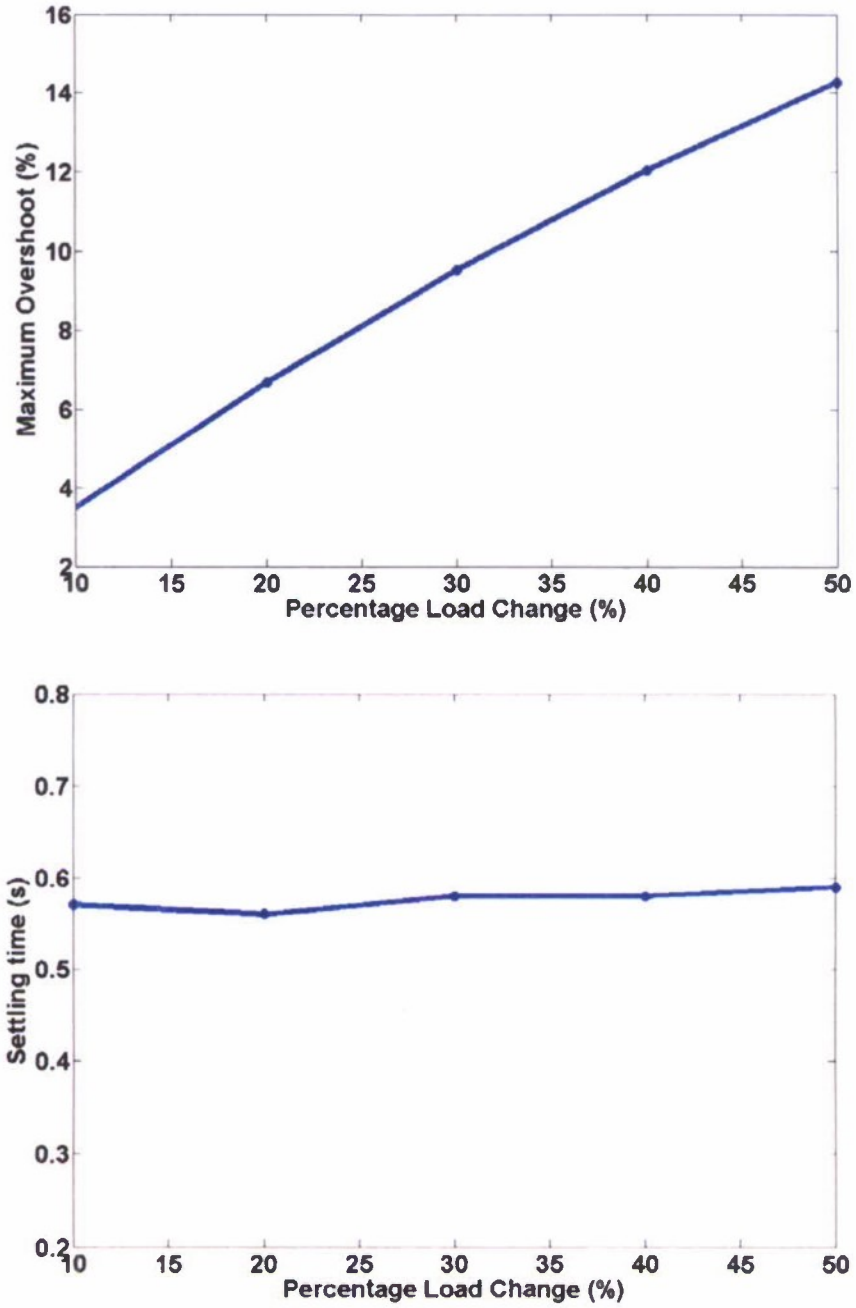

Figure 11: Gas turbine system model response to load perturbation when operating at 70% of nominal load

As with the gas turbine generator system, we examined the response of the motor generator system to transient loads. The upper plot in Figure 12 shows the generator shaft speed as a function of time when the electrical load is abruptly decreased by 20%. As was the case for the gas turbine system model, when the load is decreased, the shaft speed initially increased, and the speed oscillated as it settled back to the reference speed. The settling time remains almost

invariable (0.29s) between different sizes of load step changes applied. The lower plots in Figure 12 show the maximum speed deviation (left) and the settling time (right) as a function of magnitude of the load decrease. As was the case for the gas turbine system model, the maximum speed deviation increased as the load step increased. The settling time is relatively constant for load decreases between 10% and 50% of rated power.

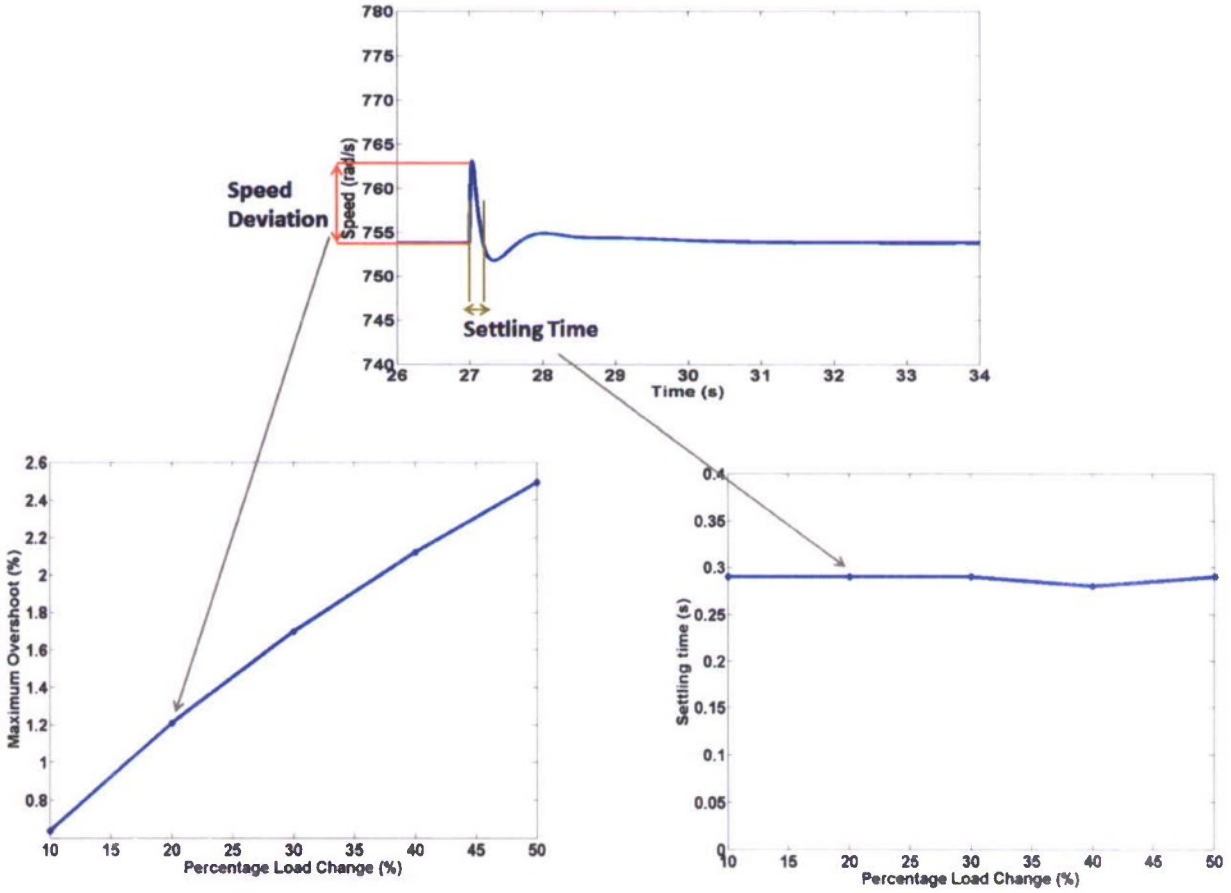

Figure 12: Motor generator system model response to load perturbation

Figure 13 shows the maximum speed deviation and the settling time as a function of magnitude of the load decrease when operating the motor generator system at 70% of nominal load. In this case, the maximum speed deviation present slightly lower values compared to the nominal case shown in Figure 12. The settling time (0.3s) is relatively constant for load decreases between 10% and 50% of rated power.

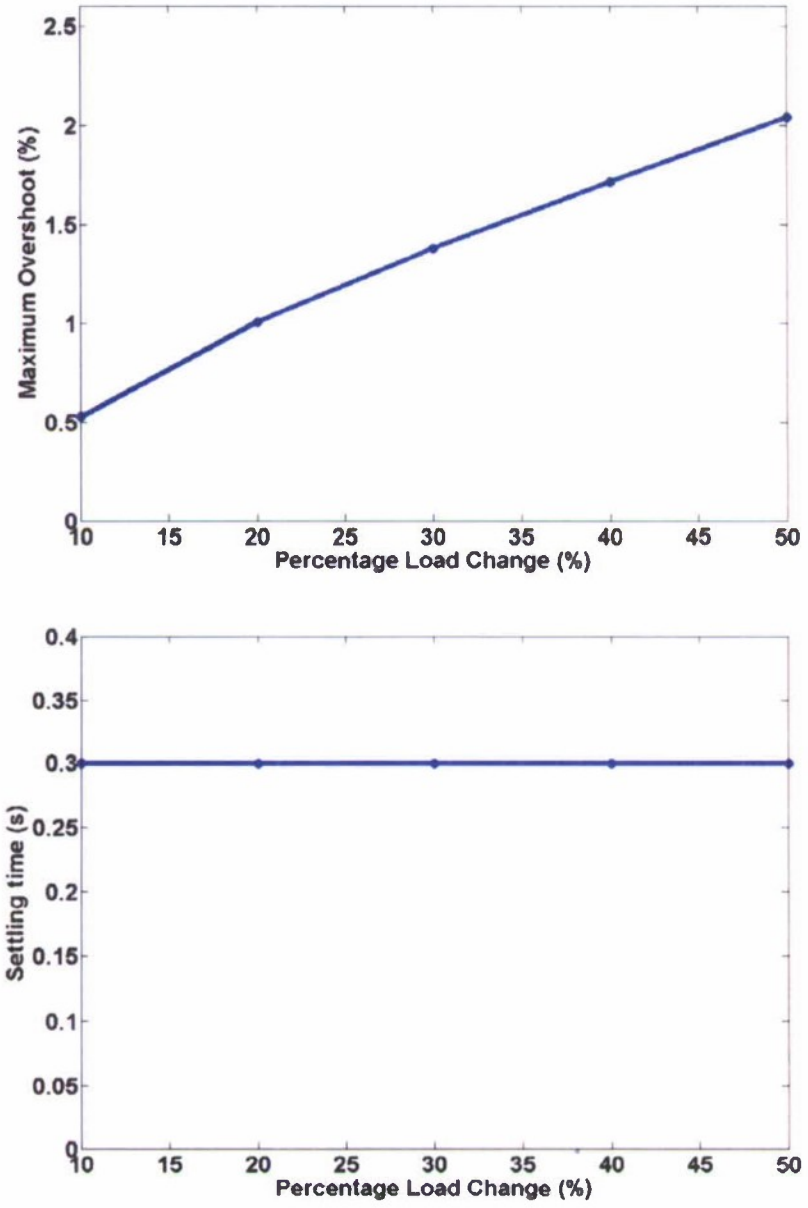

Figure 13: Motor generator system model response to load perturbation when operating at 70% of nominal load

Figure 14 compares the responses of the gas turbine generator system to that of the motor generator system when subjeeted to a 20% step load deerease. We see that the deviation of the generator speed when driven by the motor is signifieantly less than when driven by the gas turbine. There are several reasons for this. First, the larger inertia of the motor inhibits speed-up. Seeond, the motor eontrols can react nearly instantaneously to restrict power input to the motor whereas the fuel eontrol of the engine responds slightly more slowly, and even then, fuel already in the engine eontinues to burn and produee power. This behavior is eonsistent for other magnitudes of load changes (see Figure 10 and Figure 12). The more eontrollable response of the

motor compared to the gas turbine is encouraging because it indicates that the addition of appropriate controls can affect a motor speed response that is consistent with the speed response of the turbine engine.

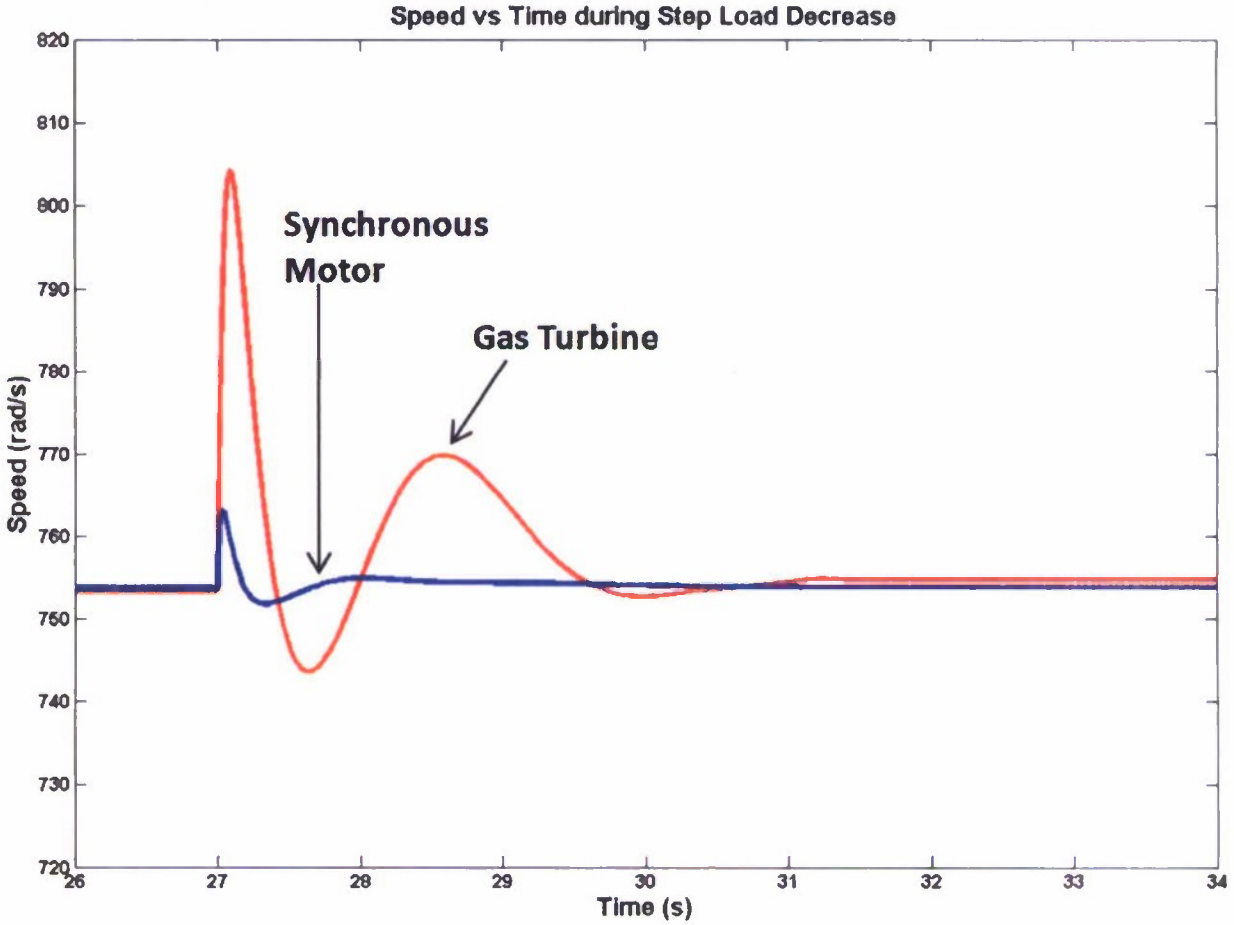

Figure 14: Comparison of response to a 20% step load decrease for the gas turbine generator system and the motor generator system

Model of the Motor Generator System Operating in Turbine Emulator Mode

The component models and vector control scheme that comprise the gas turbine emulator system model are the same as those used for the motor generator system model (synchronous motor, gear, generator, loads), but now with the addition of a gas turbine engine model within the control loop that establishes the speed reference for the motor controller. The model of the gas turbine emulator system is illustrated in Figure 15. The model-based controller compares the speed predicted by the gas turbine engine model with the speed of the motor. The gas turbine speed is determined by the throttle of the gas turbine subsystem which is regulated by the shaft torque feedback of the generator that is driven by the emulator.

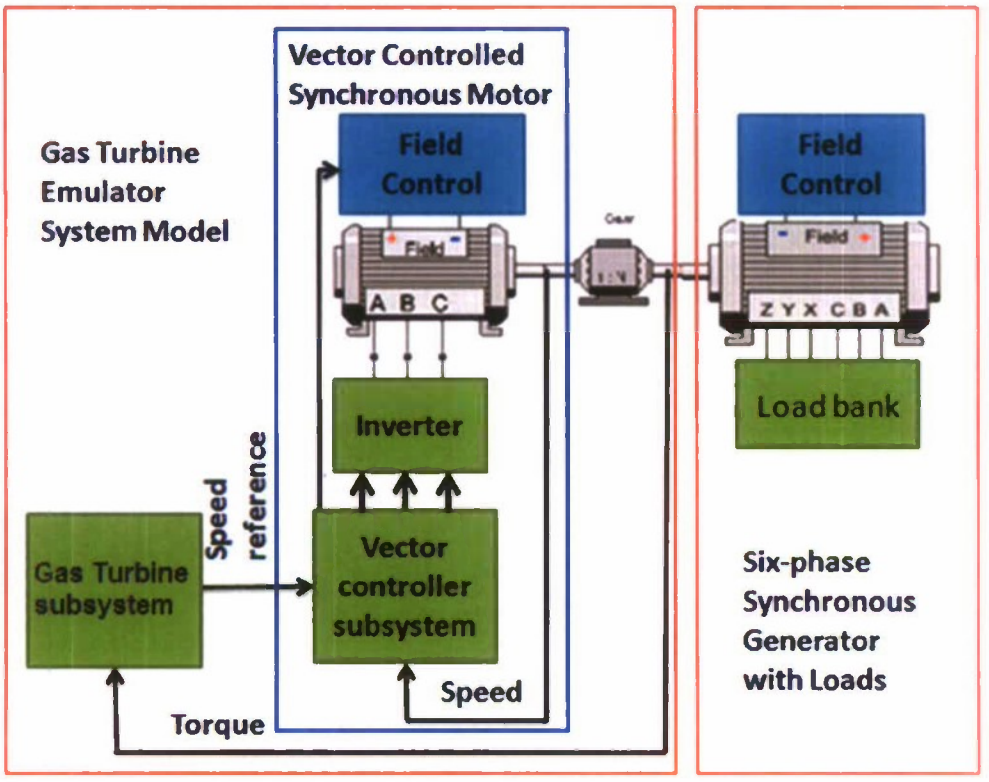

Figure 15: System model of gas turbine emulator

When the gas turbine model provides the speed reference for the emulator machine, the gas turbine generator system and the gas turbine emulator system should, ideally, exhibit identical behaviors in steady state operation and in response to system disturbances. This was tested in simulation in order to establish a proof of concept. Figure 16 compares the speed-torque characteristic of the gas turbine system with that of the gas turbine emulator system for constant speed references of 654 rad/s, 754 rad/s and 854 rad/s. At all test points, the two control loops maintained identical speeds, including in the overload range where the engine speed decreased when it reached the fuel supply limit. In this simulation, the synchronous motor was assigned an inertia of 551 kg*m^2 and the power turbine in the gas turbine system model was assigned an inertia of 1 kg*m^2. So far, we have been able to find only one gas turbine documentation file that is available online for public use and provides actual information on inertia values of the gas producer rotor and power turbine rotor. This document includes information about the Honeywell AGT1500 gas turbine for battle tanks [4], in which the gas producer rotor has an inertia value of 0.074 kg*m^2 and the power turbine rotor has an inertia value of 0.141 kg*m^2. However, it should be noted that the rated power level of the AGT1500 is only 1.12 MW. For our simulation, the rated power of the gas turbine is between 10-14MW. Since the inertia of the rotor is somewhat proportional to the rated power level we estimate that the inertia value of the power turbine can be somewhere in the range of 0.6-1.5 kg*m^2.

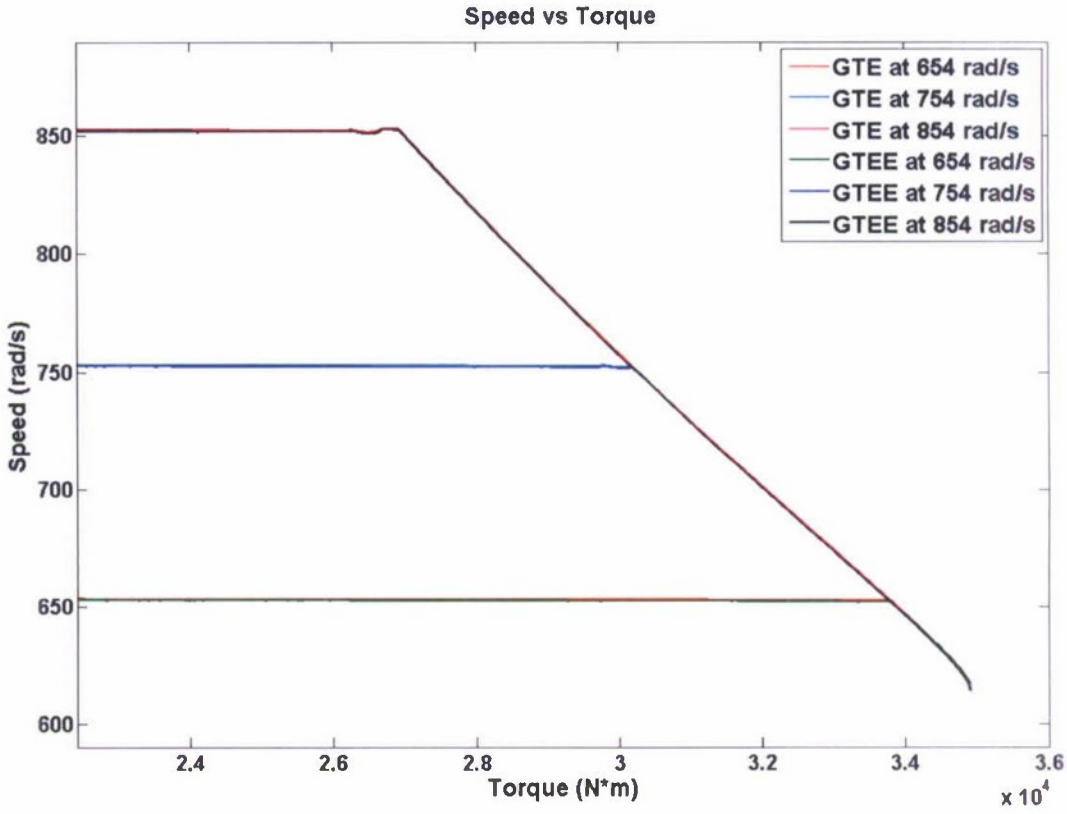

Figure 16: Comparison of steady state speed-torque characteristics of gas turbine engine and gas turbine emulator

We examined how well the gas turbine emulator system traeks the gas turbine system when the synehronous motor has an inertia of 551 kg*m^2 and the power turbine in the gas turbine system model has an inertia of 1 kg*m^2. Step load inereases and deereases were applied to the generator while operating at 14.4MW.

Figure 17 and Figure 18 eompare the generator speeds of the gas turbine emulator system to that of the gas turbine system in response to a step load inerease. In thc simulation a 20% step load increase was applied at t=22 seeonds. The figures show that the emulator motor system model traeks the oscillations of the turbine system model very aceuratcly. Thc amplitude of thc oseillations is slightly higher for the emulator system than for the gas turbine system. The maximum error is 2.975%, with error defined as:

$$Error = \frac{emulator\ speed - gas\ turbine\ speed}{gas\ turbine\ speed}$$

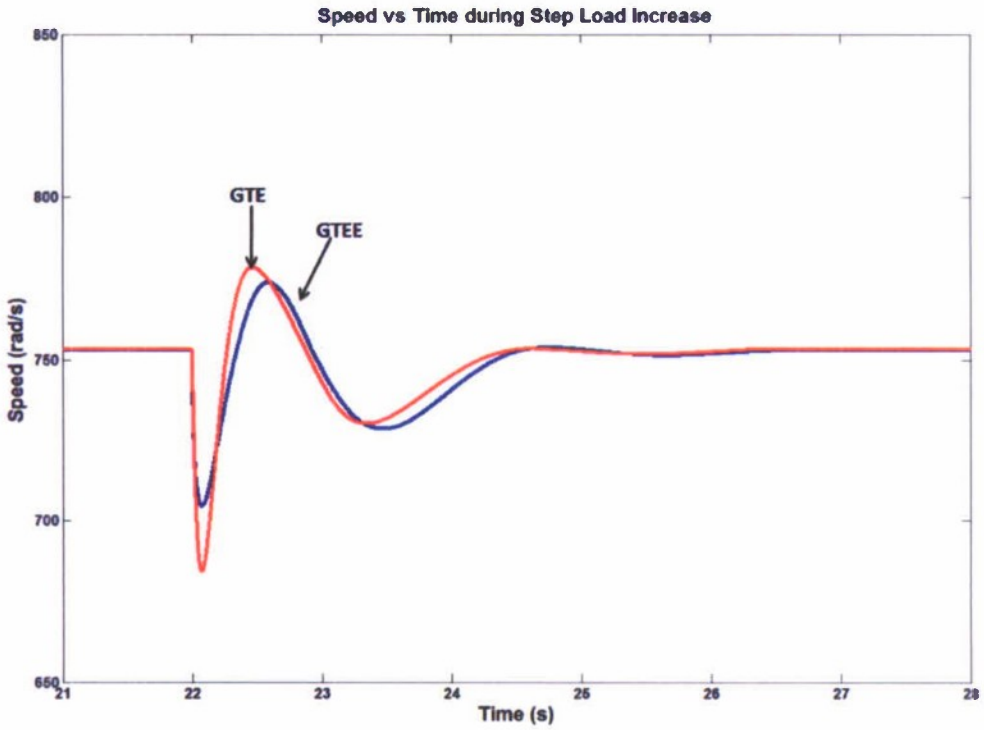

Figure 17: Comparison of rotor speeds for the gas turbine engine (GTE) and the gas turbine engine emulator (GTEE) during a step load increase

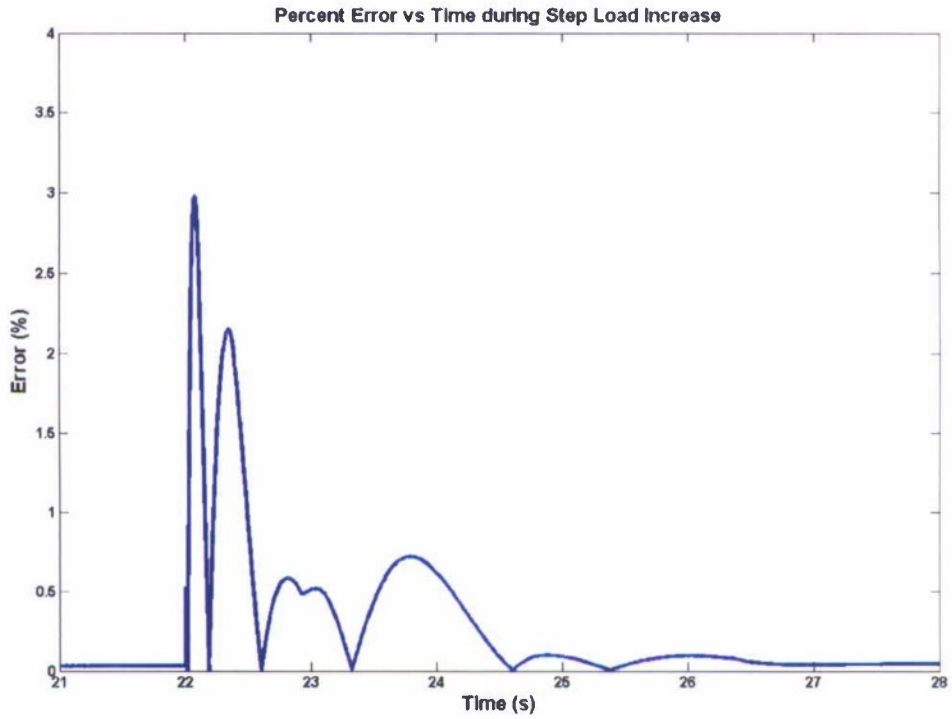

Figure 18: Error of machine speed when the rotational inertia of gas turbine emulator following a 20% increase of electric load

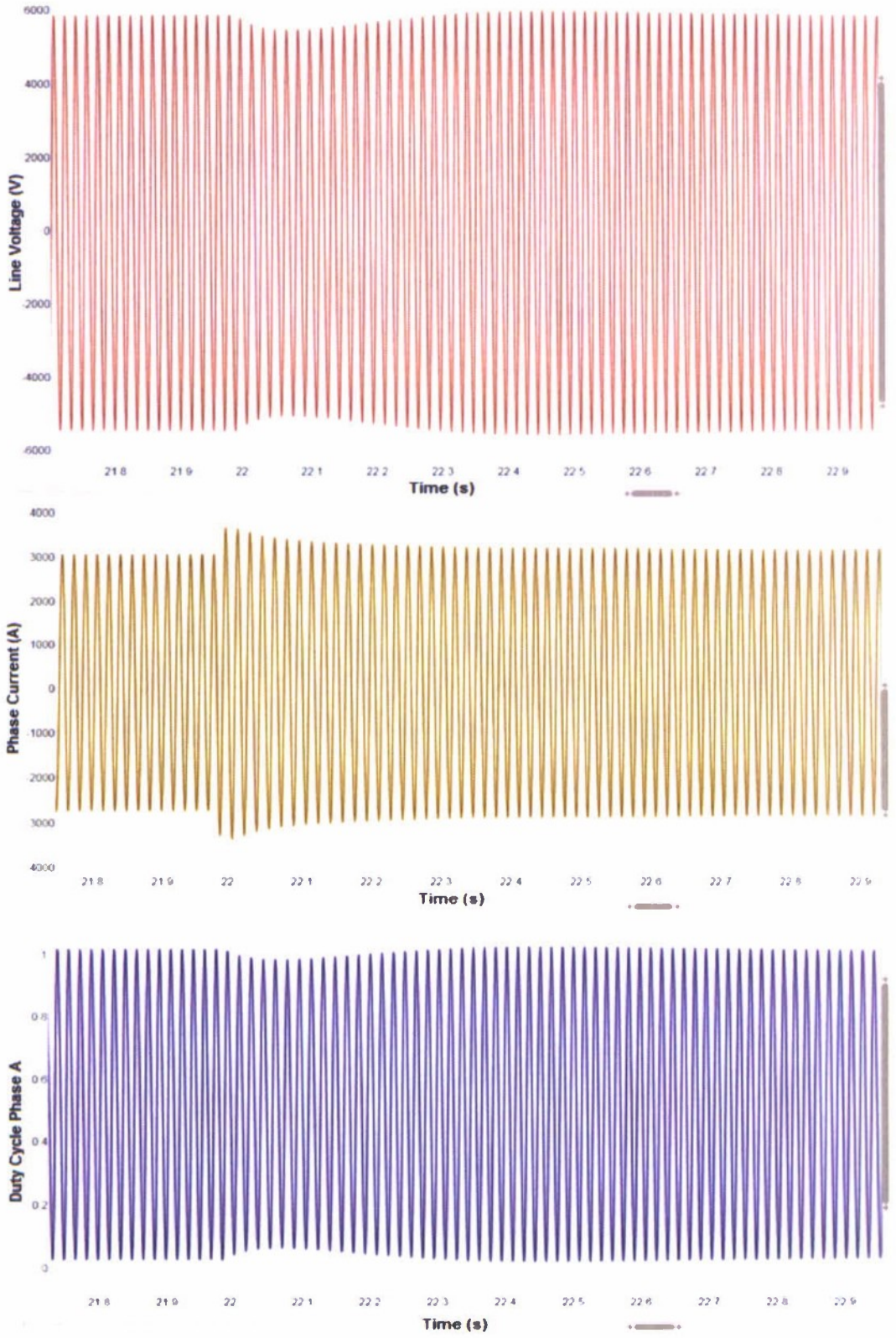

Figure 19: Line voltage, phase current and duty cycle of synchronous motor during a 20% step load increase

Figure 19 shows the line voltage, phase current and duty cycle of the synchronous motor during the 20% step load increase. As can be seen, the peak voltage of the synchronous motor is 5.88kV which corresponds to an rms line voltage of 4.16kV. At the moment the load is increased the line voltage decreases while the phase current increases. This is because more torque is applied to the motor shaft.

Figure 20 and Figure 21 compare the generator speeds of the gas turbine emulator system and the gas turbine system in response to a step load decrease. A 20% step load decrease was applied at t=22 seconds. For this case the maximum error was 1.066%, which is less than in the 20% load increase step change. This is because the synchronous motor has a larger inertia compared to the GTE inertia and more power must be extracted from the motor (regeneration mode) in order to bring the speed back to steady-state.

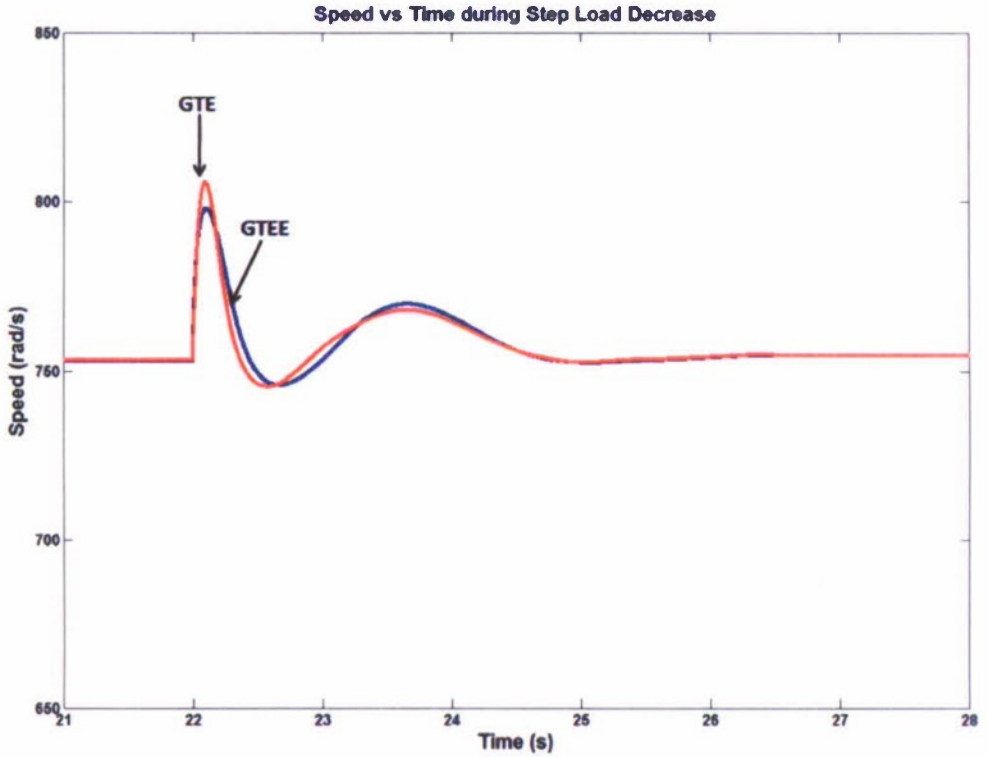

Figure 20: Comparison of speed between the gas turbine and the gas turbine emulator during a step load decrease

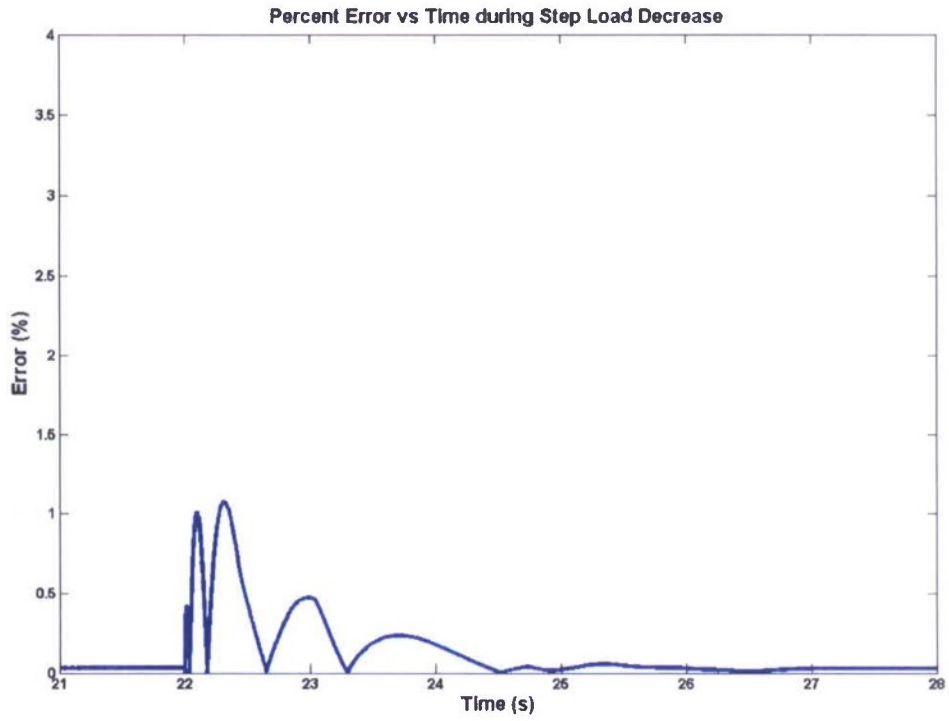

Figure 21: Error of machine speed when the rotational inertia of gas turbine emulator following a 20% decrease of electric load

Figure 22 shows the line voltage, phase current and duty cycle of the synchronous motor during the 20% step load decrease. At the moment the load is increased the line voltage slightly increases while the phase current decreases. This is because less torque is applied to the motor shaft.

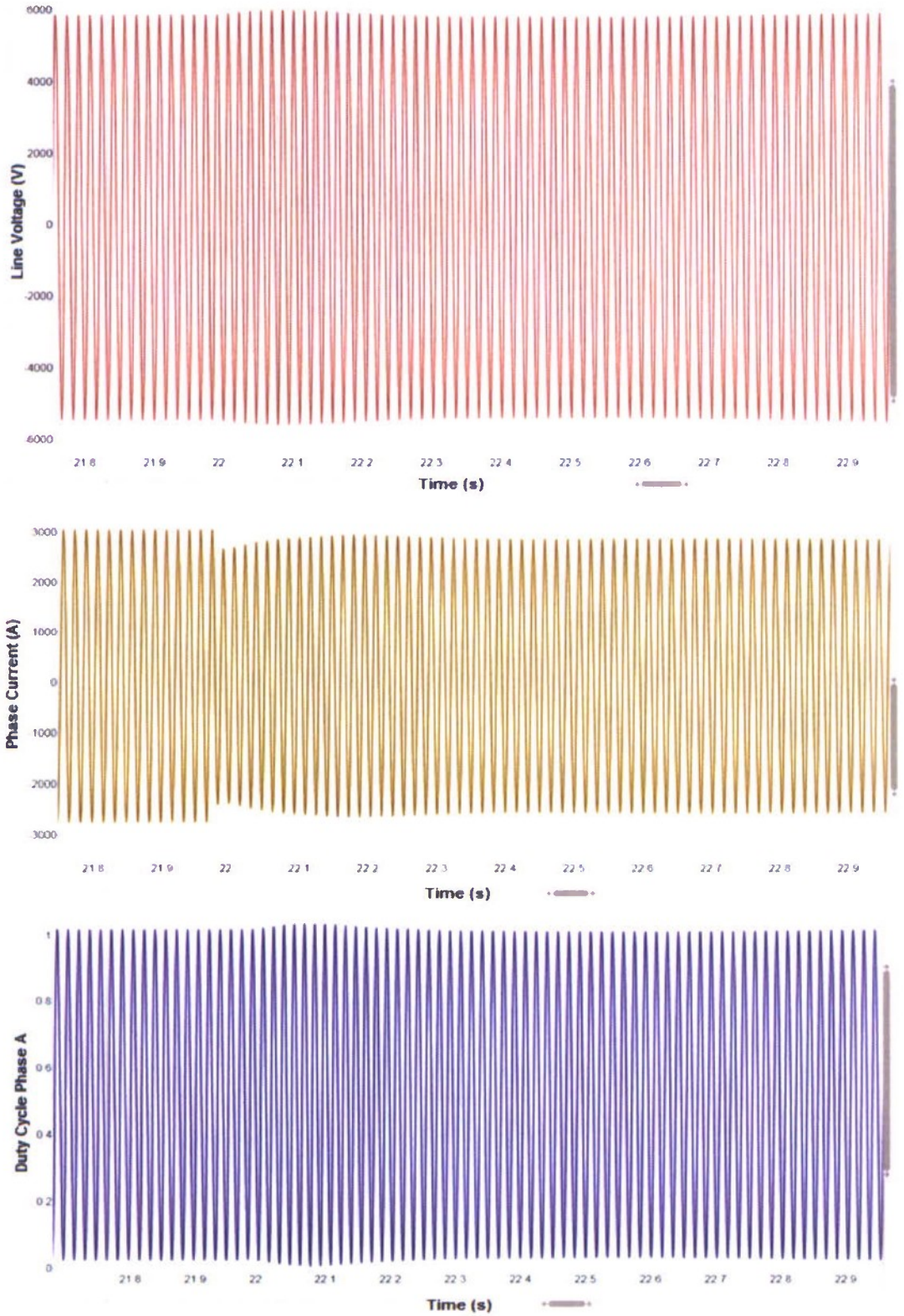

Figure 22: Line voltage, phase current and duty cycle of synchronous motor during a 20% step load decrease

POWER REQUIREMENTS FOR EMULATOR MOTOR

At some point, the power required to offset the differences in inertia between the emulator motor and that of a comparably powered gas turbine engine may be greater than the motor is capable of providing. In order to assess the power required for an electric motor to emulate a turbine engine having significantly different inertia, an analytical expression has been derived. This expression, derived from first principles, indicates that the power rating of the emulator motor (P_e) must be greater than the power of the reference gas turbine (P_{ref}) by a multiple equal to the ratio of the emulator machine inertia J_e to the reference inertia J_{ref} (where these inertias consider turbine inertia as well as the speed increase gear). This expression can be used to determine whether a particular electric machine has sufficient power, in relation to its inertia, in order emulate a specific gas turbine engine. The detailed derivation of the formula is presented in Appendix E.

$$P_e = P_{ref}\frac{J_e}{J_{ref}}$$

FUTURE WORK: EXPERIMENTAL VERIFICATION OF TRACKING CONTROL METHOD AND EMULATOR MOTOR POWER CRITERION

A series of tests are planned to demonstrate the control method and to validate the emulator motor power criterion. Figure 23 shows the system that will be implemented and tested in the laboratory in order to demonstrate the emulator motor drive system at reduced scale. The test system consists of a synchronous motor connected to a synchronous generator. The synchronous motor is controlled by a real-time speed tracking controller based on vector control and an internal model of the prime mover (turbine engine). The real-time model-based controller provides the appropriate PWM triggering pulses for the inverter switches and the buck converters that control the fields of the synchronous motor and synchronous generator. The prime mover internal model is a real-time version of the emulated prime mover and provides the appropriate speed reference for the synchronous motor speed controller. The prime mover internal model is a real-time version of the emulated prime mover simulation model and provides the appropriate speed reference for the synchronous motor speed controller. In order to realize a real-time practical hardware implementation of the GTEE a representation of the GTE model that runs in real-time is necessary. This can be achieved by using system identification techniques in order to capture the input-output behavior of a system. Due to the nonlinearity of the GTE reference model nonlinear system identification techniques will be applied. The power criterion will be validated during a transient condition by taking into account the power required by the emulated prime mover and the emulator motor as well as their respective inertia values.

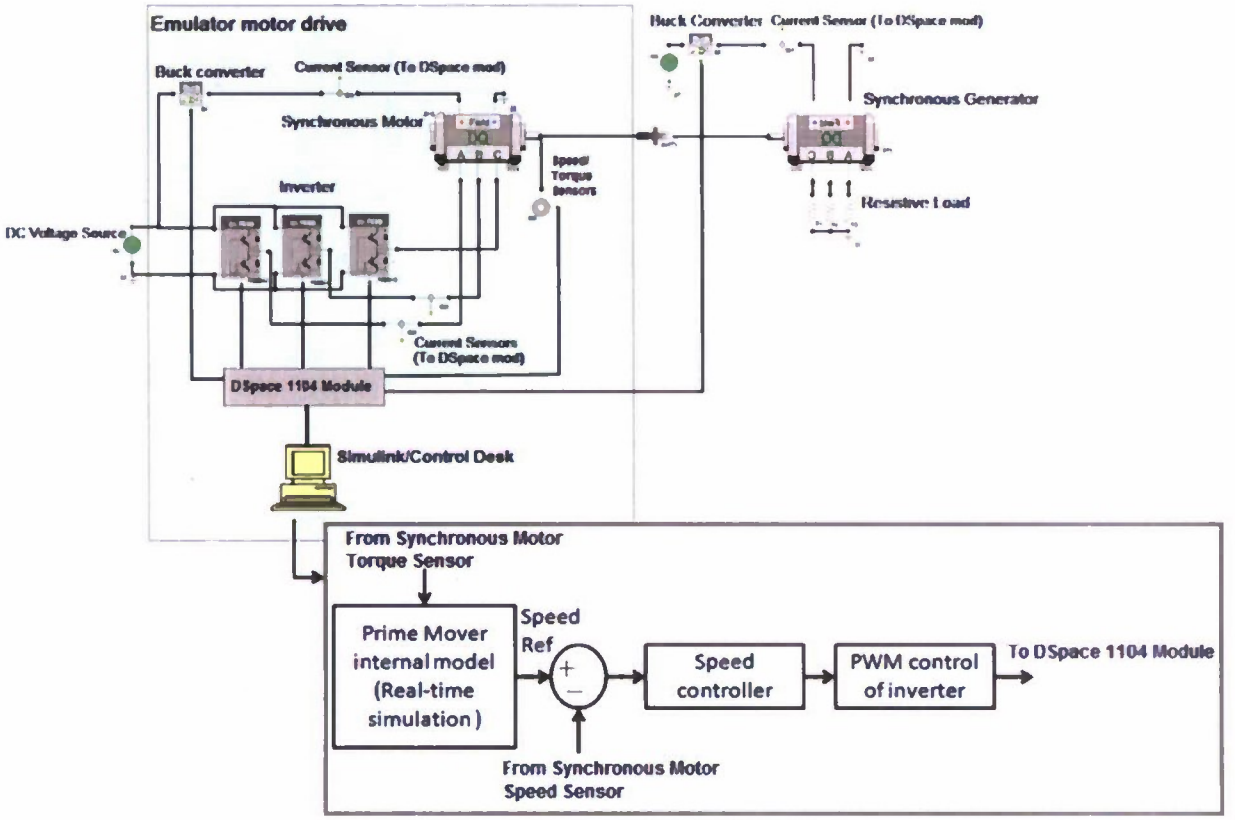

Figure 23. Schematic of hardware-in-the-loop setup of gas turbine emulator system

CONCLUSIONS

Three system models have been developed and implemented in the VTB 2009 environment:

1. Gas turbine powered generator system with user-adjustable speed referenee
2. Motor driven generator system with user-adjustable speed referenee
3. Motor-driven generator system and model-based eontrols that permit it to emulate the gas turbine generator system

In the proeess of developing these system models, new component models were designed and built for a gas turbine engine and a six phase generator. A fuel eontroller was developed for the gas turbine engine to eontrol its speed for variable torque loadings. Additionally, a eontrollable resistive load was developed to support evaluation of the system performanee.

A veetor eontroller for the synehronous motor was modeled to permit thc motor to emulate the gas turbine engine referenee model. This eontroller allows the gas turbine subsystem to provide a referenee shaft speed for the emulator motor to follow. Simulations performed using both of the system models and eomparisons of the emulator motor performanee matehed the performanee of the gas turbine elosely (error less than 2.975%).

A eriterion for power rating of a high-inertia motor to emulate a low-inertia turbine engine was derived. The eriterion will be validated in simulation and by small seale hardware tests. After verifieation the criterion ean be used to determine for the range of valid tests that ean be performed with the motor installed at the NSWC Philadelphia.

RECOMMENDATIONS FOR FUTURE WORK

Future work will foeus on enhaneing the system models, verifieation testing, and system studies using the models. The reeommended future work includes:

- **Development of experimental hardware setup:** The experimental small-seale hardware verifieation of the gas turbine emulator model will be eontinued. The hardware set-up ineludes a DSpaee 1103 module and two 250W 1800rpm synehronous motors.
- **Enhance gas turbine model:** The model will be enhaneed to inelude more eomplete maps of the turbine components. This will permit more aeeurate simulation of most engine configurations over a wide range of operating points, and will therefore make them more suitable for studies of start-up, transient loading, and engine eontrol dynamies.
- **Testing under abrupt loading conditions:** The motor drive at NSWC Philadelphia is a Robicon Perfect Harmony drive that opcratcs only in two quadrant mode, whieh means it ean only be used for delivering power to the maehine load – it eannot extraet power from the maehine. This limits how fast the maehine ean slow down, so the gas turbine may deeelerate much faster than the motor ean be decelerated. We will study

how this impacts the ability of the machine to emulate a small-inertia turbine engine under abrupt loading conditions.

- **Inclusion of a DC bus and loads:** So far, our system models have only considered a resistive AC load attached to the high speed generator. The system models can be extended to include a rectifier and DC distribution network and loads powered by the high speed generator through a rectifier, as shown in the example of Figure 24.

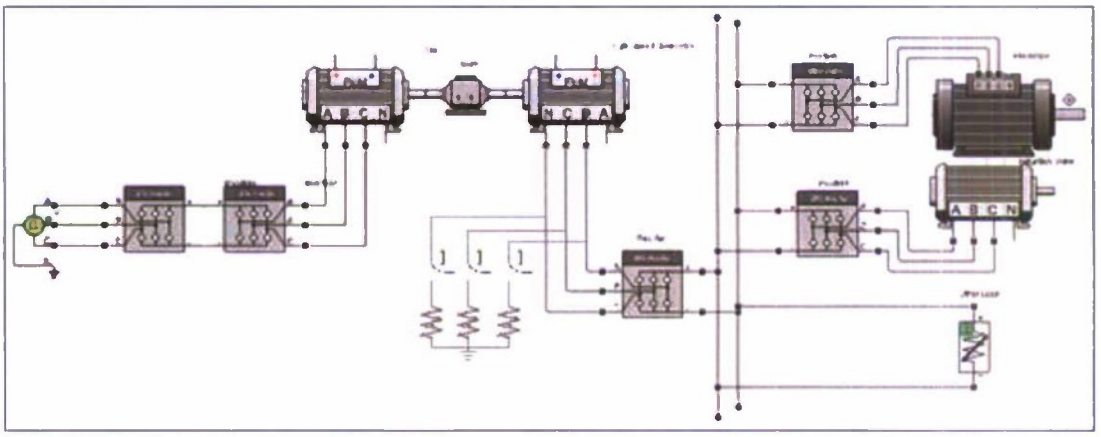

Figure 24 Inclusion of damping resistive load and DC distribution network and loads in simulation model 2

- **Design of power re-circulation configuration using two motor drives:** We will test a system configuration in which the power generated by the high speed generator is re-circulated to the input of the motor drive instead of being dissipated in a load bank. The system configuration for implementing this is shown in Figure 25.

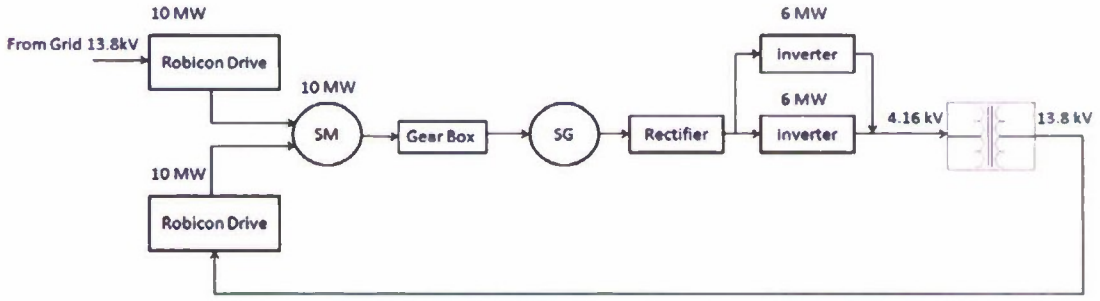

Figure 25. Configuration for re-circulating generated power

- **Analysis of faults in the power system:** We will study whether the existing or conventional, or inbuilt protection systems of the equipment are sufficient to protect against faults.

- **Intelligent control techniques for the drive system and field controls:** The vector control technique designed for the synchronous motor that emulats the gas turbine includes speed, current, flux and field current controllers which are all based on simple PI methods. The field controller of the high-speed synchronous generator is also based on a PI controller. If these simple control approaches are shown to be

inadequate to make the synchronous motor act like a gas turbine engine then we will study the design of robust controllers based on artificial intelligence techniques to improve the performance of the gas turbine emulator and field controls.

We will develop and submit to ONR a follow-on proposal to address these open issues.

REFERENCES

[1] R. F. Schiferl and C. M. Ong, "Six phase synchronous machine with ac and dc stator connections, Part I: Equivalent Circuit Representation and Steady-State Analysis" IEEE Trans. Power Appl. Syst., vol. PAS-102, pp. 2685–2693, Aug. 1983.

[2] B. K. Bose, Modern Power Electronics and AC Drives, Prentice Hall PTR, 2001, pp. 74-76, 510-515.

[3] M. Matuonto and A. Monti, "High performance field oriented control for cycloconverter-fed synchronous machine: from theory to application," Proc. EPE, Sevilla, Spain, pp. 3.458 - 3.463, 1995.

[4] AGT1500 Turbine Technology by Honeywell. Available online: http://www.honeywell.com/sites/servlet/com.merx.npoint.servlets.DocumentServlet?docid=DBFF4ECEE-AF8F-8ABE-F6D2-0E2E8F6A88FB

APPENDIX A: TWO-SHAFT GAS TURBINE SYSTEM MODEL DESCRIPTION

Gas turbine system model

The two-shaft gas turbine sub-system is illustrated in Figure A-1. To obtain 1-15 bar air pressure, a two-stage compressor design was chosen. An intercooler is applied to cool the inlet air temperature of the second compressor to achieve higher compression efficiency. The compressed air and fuel are channeled to the combustor for completely combustion. Then, the high temperature exhaust gas expands through the two shafts gas turbines whereby mechanical power is generated. The power generated by the first gas turbine is fully consumed by the compressors. Subsequent gas expansion through the power turbine produces additional mechanical power for electrical power generation. A motor is applied for system start-up, which will be cut off automatically after reaching a specific rotational speed. Important component models are described below.

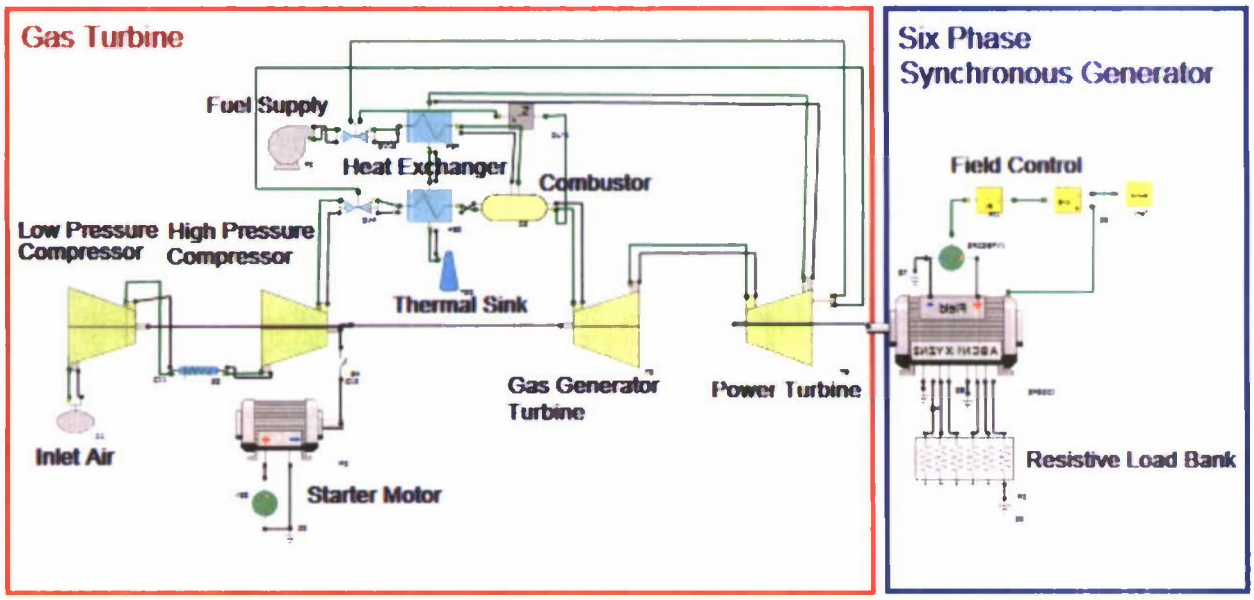

Figure A-1: Two-Shaft Gas Turbine Subsystem

Gas turbine

Thermodynamic relations and energy transfer are mainly considered for accurate prediction of the turbine characteristics. From the Euler's pump equation, the specific enthalpy coming from the fluid should be equal to the power delivered to the outer device, i.e. compressor or generator.

$$\tau_T \cdot \omega = \dot{m} \cdot Cp \cdot \eta_c \cdot T_{ci}\left(1 - \left(p_{out}/p_{in}\right)^{k-1/k}\right)$$

Compressor

A compressor is modeled to provide pressurized air for the gas turbine. Mass and energy conservation are included in the model development. The air enters the compressor rotor at the inlet with a uniform velocity and leaves at another radius with a uniform velocity. The change in momentum of the fluid is derived from the work done by the rotating rotor. The compressor characteristic equations can be described as follows.

$$\frac{d\omega}{dt} = \frac{1}{J} \cdot (\tau_t - \tau_c)$$

$$\omega \cdot \tau_c = W_c = \dot{m} \cdot \Delta h_{ideal}$$

$$\Delta p = am^2 + bm + c\omega$$

Combustor

The fuel and air are fed to the combustor, where the following combustion reaction takes place. It is assumed that fuel ($C_{12}H_{23}$,) completely reacts with the excess air.

$$C_{12}H_{23} + 17.75O_2(\dot{x}) \rightarrow 12CO_2 + 11.5H_2O \quad (\Delta h^o_{298} = -8035.6kJ/mol)$$

Heat Exchanger

This model represents a counter flow shell and tube heat exchanger, where phase change of the fluid is not considered. Under the assumption of adiabatic procedure, the total energy transfer can be written as

$$q = \dot{m}_h \cdot c_{p,h} \cdot (T_{h,i} - T_{h,o}) = \dot{m}_c \cdot c_{p,c} \cdot (T_{c,o} - T_{c,i})$$

, where ε is the overall heat transfer coefficient. For the counter flow shell and tube heat exchanger, ε can be defined as below

$$\varepsilon = 2\left\{1 + Cr + \left(1 + Cr^2\right)^{1/2} \cdot \frac{1 + \exp(-NTU \cdot \left(1 + Cr^2\right)^{1/2})}{1 - \exp(-NTU \cdot \left(1 + Cr^2\right)^{1/2})}\right\}^{-1}$$

Additional equipments necessary for operating the gas turbine sub- system include intercooler, pump, valve, thermal sink and air source. Each has been mathematically modeled.

The maximum fuel limit of the engine is a user defined parameter of the fuel valve component model.

APPENDIX B: SIX PHASE SYNCHRONOUS GENERATOR MODEL

Synchronous Generator with AVR - Used in All Testbenches

The model of a six-phase synchronous machine is [A1]. The six-phase synchronous machine is described mathematically by dividing the six stator phases into two three-phase sets displaced by an angle ε, and labeled *abc* and *xyz*. The effect of two damper windings is considered. Figure B-1 shows a schematic representation of the two stator windings, field winding and damper windings.

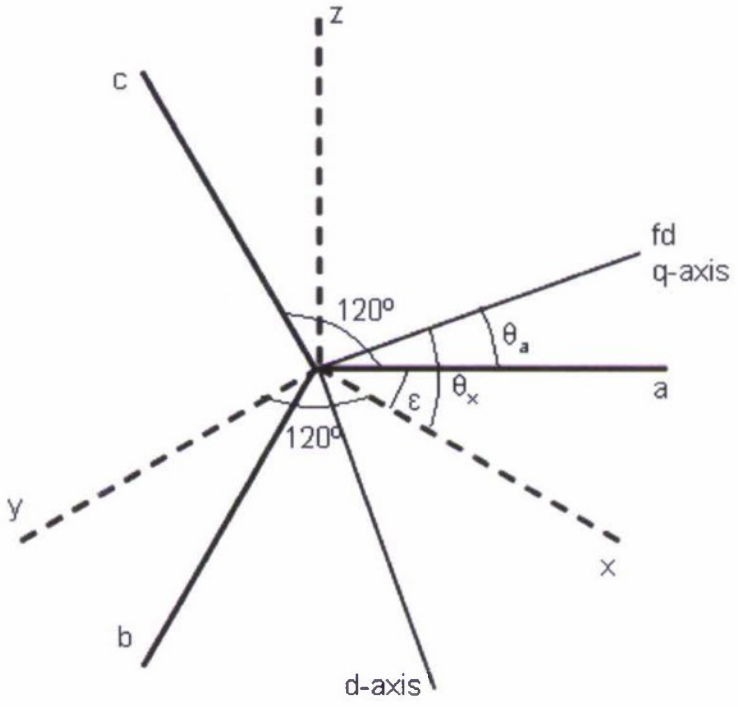

Figure B-1: Phase representation of the two stator windings, field winding and damper windings for six-phase generator

Phase *a* voltage is defined so that it is displaced by an angle of $\varepsilon = 60$ degrees from phase *x* and has 0 degree phase reference when field current flows into the field plus terminal. Phase *b* lags phase *a* by 120 degrees and phase *c* leads phase *a* by 120 degrees. Similarly, phase *y* lags phase *x* by 120 degrees and phase *z* leads phase *x* by 120 degrees.

The mathematical description was simplified by applying an orthogonal Park transformation to the stator variables in order to obtain a new set of variables, d_1, q_1, 0_1 and d_2, q_2, 0_2. The voltage equations using generator convention in this reference frame are:

$$v_{q1}^r = -r_s i_{q1}^r + w_r \lambda_{d1}^r + p\lambda_{q1}^r$$
$$v_{d1}^r = -r_s i_{d1}^r - w_r \lambda_{q1}^r + p\lambda_{d1}^r$$

$$v_{q2}^r = -r_s i_{q2}^r + w_r \lambda_{d2}^r + p\lambda_{q2}^r$$
$$v_{d2}^r = -r_s i_{d2}^r - w_r \lambda_{q2}^r + p\lambda_{d2}^r$$

$$v_{Kq} = r_{Kq} i_{Kq} + p\lambda_{Kq}$$
$$v_{Kd} = r_{Kd} i_{Kd} + p\lambda_{Kd}$$
$$v_{fr} = r_{fr} i_{fr} + p\lambda_{fr}$$

$$\lambda_{q1}^r = -L_{l1} i_{q1}^r - L_{lm}(i_{q1}^r + i_{q2}^r) + L_{ldq} i_{d2}^r + L_{mq}(-i_{q1}^r - i_{q2}^r + i_{Kq})$$
$$\lambda_{d1}^r = -L_{l1} i_{d1}^r - L_{lm}(i_{d1}^r + i_{d2}^r) - L_{ldq} i_{q2}^r + L_{mq}(-i_{d1}^r - i_{d2}^r + i_{Kd} + i_{fr})$$

$$\lambda_{q2}^r = -L_{l2} i_{q2}^r - L_{lm}(i_{q1}^r + i_{q2}^r) + L_{ldq} i_{d1}^r + L_{mq}(-i_{q1}^r - i_{q2}^r + i_{Kq})$$
$$\lambda_{d2}^r = -L_{l2} i_{d2}^r - L_{lm}(i_{d1}^r + i_{d2}^r) + L_{ldq} i_{q1}^r + L_{md}(-i_{d1}^r - i_{d2}^r + i_{Kd} + i_{fr})$$

$$\lambda_{Kq} = L_{lKq} i_{Kq} + L_{mq}(-i_{q1}^r - i_{q2}^r + i_{Kq})$$
$$\lambda_{Kd} = L_{lKd} i_{Kd} + L_{md}(-i_{d1}^r - i_{d2}^r + i_{Kd} + i_{fr})$$
$$\lambda_{fr} = L_{lfr} i_{fr} + L_{md}(-i_{d1}^r - i_{d2}^r + i_{Kd} + i_{fr})$$

$$T_{em} = i_{q1}^r \lambda_{d1}^r + i_{q2}^r \lambda_{d2}^r - i_{d1}^r \lambda_{q1}^r - i_{d2}^r \lambda_{q2}^r$$

$$T_m = J\frac{d\omega}{dt} + T_e$$

References

[A1] R. F. Schiferl and C. M. Ong, "Six phase synchronous machine with ac and dc stator connections, Part I: Equivalent Circuit Representation and Steady-State Analysis" IEEE Trans. Power Appl. Syst., vol. PAS-102, pp. 2685–2693, Aug. 1983.

APPENDIX C: MODEL 2: SYNCHRONOUS MOTOR MODEL

The synchronous machine model works for a 3-phase system. The model has ABC terminals to connect to the outside electrical system. It also has an excitation winding on the D axis and two damping windings on both D and Q axis. If the input power is electrical power and the load is a mechanical load, the model works as a motor. If the input power is mechanical power and the load is an electrical load, the model works as a generator. This model uses a physics based equation under the assumption that all the material inside the machine is ideal. There is no flux saturation in the iron. All the energy is stored in the air gap.

Mathematical Description:

$$v_q = r_s i_{qs} + \omega \lambda_{ds} + p\lambda_{qs}$$

$$v_d = r_s i_{ds} - \omega \lambda_{qs} + p\lambda_{ds}$$

$$v_f = r_f i_{df} + p\lambda_{fr}$$

$$0 = r_{qr} i_{qr} + p\lambda_{qr}$$

$$0 = r_{dr} i_{dr} + p\lambda_{dr}$$

$$\lambda_{qs} = L_{qs} i_{qs} + L_{mq} i_{qr}$$

$$\lambda_{ds} = L_{ds} i_{ds} + L_{md} i_{dr} + L_{md} i_{df}$$

$$\lambda_{fr} = L_{df} i_{df} + L_{md} i_{dr} + L_{md} i_d$$

$$T_e = \lambda_d i_q - \lambda_q i_d$$

$$T_m = J\frac{d\omega}{dt} + T_e$$

where,

v_q: *q axis stator voltage*

v_d: *d axis stator voltage*

v_f: *excitation voltage*

λ_{qs}: *q axis stator flux*

λ_{ds}: *d axis stator flux*

λ_{fr}: *field flux*

T_e: *electromagnetic torque*

T_m: *mechanical torque*

θ: *mechanical shaft rotation angle*

ω: *mechanical shaft rotation speed*

r_s: *stator resistance*

r_f: *field resistance*

L_{qs}: *q axis stator inductance*

L_{ds}: *d axis stator inductance*

L_{mq}: *q axis mutual inductance*

L_{md}: *d axis mutual inductance*

L_{df}: *field inductance*

P: *poles*

J: *inertia*

APPENDIX D: VECTOR CONTROL SCHEME

The speed control of the synchronous motor, which is based on the concepts of vector control, has been improved to include the field current and flux controllers, and the flux observer. The complete control scheme is shown in Figure C-1.

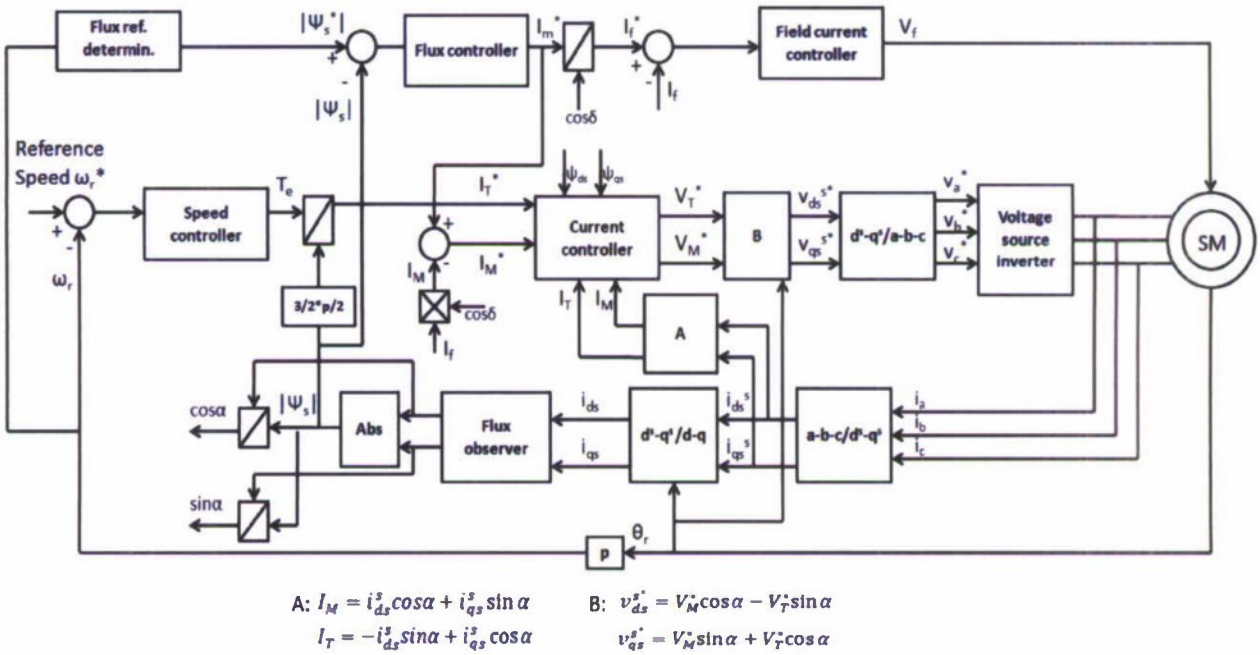

Figure D- 1. Vector control scheme of the synchronous motor emulating a gas turbine engine

A description of the vector control scheme for the synchronous motor is given as follows:

Flux controller: The monitored rotor speed serves as input to the flux reference determination block, the output of which is a constant value of the stator flux reference ψ_s^* when the motor is operated below base speed and a reduced value of the stator flux when the motor is operated above base speed. The stator flux reference is compared with the actual value of the stator flux ψ_s obtained from the flux observer and their difference is fed into the flux controller, which is a PI controller. The output of the flux controller is the reference value of the magnetizing current I_m^* required to establish the desired ψ_s.

Field current controller: At steady-state, the field current I_f is related to the magnetizing current I_m by the relation:

$$I_f = \frac{I_m}{\cos\delta}$$

, where δ is the angle between the I_m and I_f phasors. This control equation establishes the field current command I_f^*, which is then compared to the actual value of the field current I_f. The field current controller generates the field voltage command v_f through a PI controller.

Flux observer: An observer is usually implemented to reconstruct the inaccessible states in a system. The flux observer allows the calculation of the stator flux $|\Psi_s|$ by using known variables such as the machine parameters and the currents, which are measurable. The flux observer defined in the first two following equations, in which the d a q-axis stator flux components, Ψ_{ds} and Ψ_{qs},respectively, are described in terms of machine parameters and currents, applies to a synchronous machine with one d and q axis damper windings. In this project, the machine model describes a round rotor synchronous machine and hence it has one d axis and 2 q axis damper windings. Subsequently, the mathematical expression for Ψ_{ds} remains the same but the one for Ψ_{qs} was recalculated and is defined by the third equation shown.

$$\Psi_{ds} = L_{md}(I_f + + i_{ds}) \frac{1 + p(\frac{L_{lkd}}{R_{kd}})}{1 + p(\frac{L_{md} + L_{lkd}}{R_{kd}})}$$

$$\Psi_{qs} = L_{mq} i_{qs} \frac{1 + p(\frac{L_{lkq}}{R_{kq}})}{1 + p(\frac{L_{mq} + L_{lkq}}{R_{kq}})}$$

$$\Psi_{qs} = i_{qs} \frac{(L_{mq}L_{lk1q}L_{lk2q})p^2 + L_{mq}(R_{1q}L_{lk2q} + R_{2q}L_{lk1q})p + L_{aq}R_{k2q}R_{k1q}}{(L_{mq}(L_{lk1q} + L_{lk2q}) + L_{lk1q}L_{lk2q})s^2 + \left(L_{lk2q}R_{k1q} + L_{lk1q}R_{k2q} + L_{mq}(R_{k1q} + R_{k2q})\right)p + R_{k1q}R_{k2q}}$$

The command current I_T^* can then be calculated using the following equation:

$$I_T = \frac{T_e}{3\frac{P}{2}\psi_s}$$

The output of the flux observer yields the stator flux $|\psi_s|$, cosα and sinα:

$$\varphi_s = \sqrt{\varphi_{ds}^{s2} + \varphi_{qs}^{s2}}$$

$$\sin\alpha = \frac{\varphi_{qs}^{s}}{\varphi_s}$$

$$\cos\alpha = \frac{\varphi_{ds}^{s}}{\varphi_s}$$

Speed controller: The reference rotor speed and the monitored rotor speed are compared and their difference is fed into a PI controller, which yields the reference value of the electromagnetic torque T_e.

Current controller: The flux component of the stator current I_M^* is given by the relation:

$$I_M^* = I_m^* - I_f \cos\delta$$

At the steady state condition it is expected that $I_M^* = 0$ since the required magnetizing current is produced only by the field winding. The command currents I_T^* and I_M^* are compared with the respective feedback currents and the errors generate the voltage commands v_T^* and v_M^* through the PI controllers. These voltage signals are then transformed to the three-phase stationary reference frame to generate the phase voltage commands of the inverter.

Axes transformation:

The 3->2 block first transforms the three-phase stationary reference frame (abc) variables into two-phase stationary reference frame variables (d^s-q^s) and then transforms these to a synchronously rotating reference frame (d^e-q^e). These transformations are given as:

$$\begin{bmatrix} i_{qs}^s \\ i_{ds}^s \end{bmatrix} = \frac{2}{3}\begin{bmatrix} 1 & -\frac{1}{2} & -\frac{1}{2} \\ 0 & -\frac{\sqrt{3}}{2} & \frac{\sqrt{3}}{2} \end{bmatrix}\begin{bmatrix} i_{as} \\ i_{bs} \\ i_{cs} \end{bmatrix}$$

$$\begin{bmatrix} i_{qs} \\ i_{ds} \end{bmatrix} = \begin{bmatrix} \cos\theta_e & -\sin\theta_e \\ \sin\theta_e & \cos\theta_e \end{bmatrix}\begin{bmatrix} i_{qs}^s \\ i_{ds}^s \end{bmatrix}$$

Currents I_T and I_M can be obtained by the following transformation:

$$I_M = i_{ds}^s cos\alpha + i_{qs}^s \sin\alpha$$
$$I_T = -i_{ds}^s sin\alpha + i_{qs}^s \cos\alpha$$

The 2->3 block performs the inverse transformations included in the 3->2 block.

APPENDIX E: DERIVATION OF THE POWER REQUIREMENT FORMULA

The power criterion is derived from the torque equations defined for the emulator motor, (1), and the gas turbine engine, (2). The terms in (1), (2) and (3) are defined in Table 1.

$$T_E = J_E \frac{d\omega_E}{dt} + B_E \omega_E + T_L \quad (1)$$

$$T_{GT} = J_{GT} \frac{d\omega_{GT}}{dt} + B_{GT} \omega_{GT} + T_L \quad (2)$$

Power equals torque (T) times rotational speed (w):

$$P = Tw \quad (3)$$

Torque equals the moment of inertia (J) times the change in speed with time (dw/dt) if rotational losses are neglected and the torque load (T_L) is zero. Substituting this into (3) yields.

$$P = J \frac{dw}{dt} w \quad (4)$$

Rearranging (4) to solve for (dw/dt) yields.

$$\frac{dw}{dt} = \frac{P}{Jw} \quad (5)$$

It is desired that the reference motor and the emulator motor change in speed with time to be equal.

$$\frac{dw_{GT}}{dt} = \frac{dw_E}{dt} \quad (6)$$

Substituting (5) into (6) gives:

$$\frac{P_{GT}}{J_{GT} w_{GT}} = \frac{P_E}{J_E w_E} \quad (7)$$

Since it is also desired that $w_{GT} = w_E$, w_{GT} and w_E drop out of the equation producing:

$$\frac{P_E}{P_{GT}} = \frac{J_E}{J_{GT}} \quad (8)$$

Thus ratio of the emulator power to the reference power is equal to the ratio of the emulator inertia to the reference inertia.

If the effect of rotational losses and torque load is included the power requirement for the emulator is:

$$P_E = P_{GT} \frac{J_E}{J_{GT}} + \left(\frac{B_E}{B_{GT}} - \frac{J_E}{J_{GT}}\right) B_{GT} \omega^2 + \left(1 - \frac{J_E}{J_{GT}}\right) T_L \omega \quad (10)$$

TABLE 1

Parameter definitions of Eqn. (1), (2) and (3)

Parameter name	Parameter definition
T_E	Emulator motor torque
T_{GT}	Gas turbine torque
J_E	Emulator motor and load inertia
J_{GT}	Gas turbine and load inertia
B_E	Emulator motor damping coefficient
B_{GT}	Gas turbine damping coefficient
ω_E	Emulator motor speed
ω_{GT}	Gas turbine speed
T_L	Load torque
P_E	Emulator motor power
P_{GT}	Gas turbine power